Circulation Research

ORIGINAL RESEARCH

Ca^{2+}-CaM Dependent Inactivation of RyR2 Underlies Ca^{2+} Alternans in Intact Heart

Jinhong Wei, Jinjing Yao, Darrell Belke, Wenting Guo, Xiaowei Zhong, Bo Sun, Ruiwu Wang, John Paul Estillore, Alexander Vallmitjana, Raul Benitez, Leif Hove-Madsen, Enrique Alvarez-Lacalle, Blas Echebarria, S.R. Wayne Chen

RATIONALE: Ca^{2+} alternans plays an essential role in cardiac alternans that can lead to ventricular fibrillation, but the mechanism underlying Ca^{2+} alternans remains undefined. Increasing evidence suggests that Ca^{2+} alternans results from alternations in the inactivation of cardiac RyR2 (ryanodine receptor 2). However, what inactivates RyR2 and how RyR2 inactivation leads to Ca^{2+} alternans are unknown.

OBJECTIVE: To determine the role of CaM (calmodulin) on Ca^{2+} alternans in intact working mouse hearts.

METHODS AND RESULTS: We used an in vivo local gene delivery approach to alter CaM function by directly injecting adenoviruses expressing CaM-wild type, a loss-of-function CaM mutation, CaM (1–4), and a gain-of-function mutation, CaM-M37Q, into the anterior wall of the left ventricle of RyR2 wild type or mutant mouse hearts. We monitored Ca^{2+} transients in ventricular myocytes near the adenovirus-injection sites in Langendorff-perfused intact working hearts using confocal Ca^{2+} imaging. We found that CaM-wild type and CaM-M37Q promoted Ca^{2+} alternans and prolonged Ca^{2+} transient recovery in intact RyR2 wild type and mutant hearts, whereas CaM (1–4) exerted opposite effects. Altered CaM function also affected the recovery from inactivation of the L-type Ca^{2+} current but had no significant impact on sarcoplasmic reticulum Ca^{2+} content. Furthermore, we developed a novel numerical myocyte model of Ca^{2+} alternans that incorporates Ca^{2+}-CaM-dependent regulation of RyR2 and the L-type Ca^{2+} channel. Remarkably, the new model recapitulates the impact on Ca^{2+} alternans of altered CaM and RyR2 functions under 9 different experimental conditions. Our simulations reveal that diastolic cytosolic Ca^{2+} elevation as a result of rapid pacing triggers Ca^{2+}-CaM dependent inactivation of RyR2. The resultant RyR2 inactivation diminishes sarcoplasmic reticulum Ca^{2+} release, which, in turn, reduces diastolic cytosolic Ca^{2+}, leading to alternations in diastolic cytosolic Ca^{2+}, RyR2 inactivation, and sarcoplasmic reticulum Ca^{2+} release (ie, Ca^{2+} alternans).

CONCLUSIONS: Our results demonstrate that inactivation of RyR2 by Ca^{2+}-CaM is a major determinant of Ca^{2+} alternans, making Ca^{2+}-CaM dependent regulation of RyR2 an important therapeutic target for cardiac alternans.

GRAPHIC ABSTRACT: A graphic abstract is available for this article.

Key Words: calmodulin ■ heart ■ mutation ■ ryanodine ■ sarcoplasmic reticulum

Meet the First Author, see p 453

Cardiac alternans is a beat-to-beat alternation in the magnitude of a cardiac parameter such as the force of contraction (mechanical alternans), a component of the ECG waveform (eg, T-wave alternans), the action potential (AP) duration (APD alternans), or the amplitude of the cytosolic Ca^{2+} transient (Ca^{2+} alternans). Importantly, one or more types of these cardiac alternans are frequently observed in various experimental settings and in patients with ischemic heart disease and heart failure.[1,2] Therefore, cardiac alternans is a well-recognized risk factor for ventricular fibrillation and sudden cardiac death.[2–6] However, the molecular mechanisms underlying cardiac alternans remain incompletely understood.

Correspondence to: S.R. Wayne Chen, PhD, Department of Physiology and Pharmacology, Libin Cardiovascular Institute, 3330 Hospital Dr NW, Calgary, Alberta T2N 4N1, Canada. Email swchen@ucalgary.ca

The Data Supplement is available with this article at https://www.ahajournals.org/doi/suppl/10.1161/CIRCRESAHA.120.318429.

For Disclosures, see page e81.

Circulation Research is available at www.ahajournals.org/journal/res

ORIGINAL RESEARCH

Novelty and Significance

What Is Known?

- Calcium alternans has a primary role in the genesis of cardiac alternans, a well-known risk factor for ventricular fibrillation and sudden cardiac death.
- Calcium alternans is believed to result from beat-to-beat alternation in sarcoplasmic reticulum calcium cycling.
- The recovery from inactivation of cardiac RyR2 (ryanodine receptor 2)-mediated sarcoplasmic reticulum calcium release critically determines the induction of calcium alternans, but the molecular basis of RyR2 inactivation is unknown.

What New Information Does This Article Contribute?

- Calcium/calmodulin-dependent inactivation of RyR2 is a major determinant of calcium alternans in intact hearts.
- Calcium/calmodulin inactivation of RyR2 is driven by fast pacing-induced diastolic cytosolic calcium elevation.
- Regulation of RyR2 by calcium/calmodulin represents an important therapeutic target for cardiac alternans.

Ca^{2+} alternans play a primary role in the genesis of cardiac alternans, a beat-to-beat alternation in cardiac electrical activity and contraction and a well-recognized risk factor for ventricular fibrillation. Despite its critical significance, the molecular mechanism underlying Ca^{2+} alternans remains a mystery for decades. Recent studies have suggested that Ca^{2+} alternans results from beat-to-beat alternations in the inactivation/refractoriness of the sarcoplasmic reticulum Ca^{2+} release channel (the cardiac ryanodine receptor, RyR2). However, the molecular basis of RyR2 inactivation is largely unknown. Here, we demonstrate that Ca^{2+}-CaM (calmodulin) dependent inhibition of RyR2 underlies beat-to-beat inactivation of RyR2 that drives Ca^{2+} alternans in intact working hearts. Based on this new finding, we developed a novel numerical myocyte model of Ca^{2+} alternans. Our simulation analyses reveal that fast-pacing induces diastolic cytosolic Ca^{2+} elevation that triggers beat-to-beat Ca^{2+}-CaM-dependent inactivation of RyR2, which, in turn, causes beat-to-beat alternations in diastolic cytosolic Ca^{2+}, RyR2 inactivation, RyR2-mediated Ca^{2+} release, and thus Ca^{2+} alternans. Our experimental and computational work provides fundamental new insights into the induction and progression of fast-pacing induced Ca^{2+} alternans, making Ca^{2+}-CaM-dependent regulation of RyR2 a promising target for suppressing cardiac alternans, ventricular fibrillation, and sudden cardiac death.

Nonstandard Abbreviations and Acronyms

APD	action potential duration
Ca^{2+}_{cyto}	cytoplasmic Ca^{2+}
CaM (1–4)	a loss-of-function CaM mutation with all 4 EF-motifs mutated
CaM	calmodulin
CaM-M37Q	a gain-of-function mutation Met37Asn
GFP	green fluorescence protein
GOF	gain-of-function
I_{Ca}	L-type Ca^{2+} current
$J_{release}$	RyR2 mediated Ca^{2+} release
J_{uptake}	SR Ca^{2+} uptake
RyR2	ryanodine receptor type 2
SR	sarcoplasmic reticulum
WT	wild type

Among different forms of cardiac alternans, Ca^{2+} alternans is thought to play a primary role in the genesis of cardiac alternans.[7–12] For instance, Ca^{2+} alternans could still be observed in cardiomyocytes that were voltage-clamped, suggesting that APD alternans is not required for Ca^{2+} alternans.[8] Furthermore, Wan et al[13] simultaneously recorded the membrane potential and Ca^{2+} transients in isolated cardiomyocytes and showed that Ca^{2+} alternans occurred in the absence of APD alternans, whereas APD alternans did not occur without Ca^{2+} alternans. An increased body of evidence supports the notion that Ca^{2+} dysregulation has a primary role in cardiac alternans.[7–11,13–17] Therefore, understanding how Ca^{2+} alternans occurs is key to the understanding of cardiac alternans and the treatment of ventricular fibrillation and sudden cardiac death.

It is generally believed that Ca^{2+} alternans results from altered intracellular Ca^{2+} cycling.[11,18–21] It is well established that the amplitude of the Ca^{2+} transient in cardiomyocytes as a result of Ca^{2+}-induced Ca^{2+} release depends on (1) the L-type Ca^{2+} current (I_{Ca}), (2) the sarcoplasmic reticulum (SR) Ca^{2+} content, and (3) the activity of RyR2 (ryanodine receptor 2).[18] Studies have consistently shown that there are no beat-to-beat alternations in the peak I_{Ca} during Ca^{2+} alternans.[17,22,23] Furthermore, beat-to-beat alternation in the peak I_{Ca}, when it was observed, was found to be a consequence rather than a cause of Ca^{2+} alternans.[24,25] These observations suggest that alternation

in the peak I_{Ca} is unlikely to be a primary cause of Ca^{2+} alternans. Similarly, since Ca^{2+} alternans were observed in the presence or absence of beat-to-beat alternations in SR Ca^{2+} content,[9,23] it is also unlikely that alternation in SR Ca^{2+} content is a primary cause of Ca^{2+} alternans. This leaves the activity of RyR2 as a pivotal candidate for the occurrence of Ca^{2+} alternans. Consistent with this view, pharmacological and experimental interventions and genetic manipulations that alter the activity of RyR2 markedly affect the propensity for Ca^{2+} alternans.[22,26–28]

It has been suggested that the refractoriness of RyR2 or the recovery of RyR2 from some kind of inactivation contributes to the induction of Ca^{2+} alternans.[16,23,27,29,30] In support of these experimental observations, numerical modeling studies have also shown the importance of RyR2 refractoriness in the induction of Ca^{2+} alternans.[20,31–33] However, despite its fundamental significance, the molecular basis of RyR2 inactivation/refractoriness that contributes to Ca^{2+} alternans remains unknown.

During SR Ca^{2+} release, the released Ca^{2+} binds to CaM, and the Ca^{2+}-CaM complex inhibits RyR2.[34–36] Hence, Ca^{2+}-CaM-dependent inactivation of RyR2 follows each SR Ca^{2+} release. CaM also plays an important role in the termination of RyR2-mediated Ca^{2+} release.[37] Expression of CaM-wild type (WT) promotes the termination of Ca^{2+} release in HEK293 cells expressing RyR2, whereas the Ca^{2+}-insensitive CaM mutation, CaM (1–4) that disables all 4 EF-hand Ca^{2+} binding motifs, suppresses the termination of Ca^{2+} release.[37] CaM has also been shown to affect the refractoriness of SR Ca^{2+} release.[38] Thus, by modulating the termination and refractoriness of SR Ca^{2+} release, CaM likely plays a key role in the relaxation of cardiac muscle. Notwithstanding its physiological significance, the role of CaM in the induction of Ca^{2+} alternans is completely undefined.

In the present study, we assessed the role of CaM in the induction of Ca^{2+} alternans in intact working hearts. We performed laser-scan confocal Ca^{2+} imaging of cardiomyocytes in intact WT and RyR2 mutant hearts infected in vivo with adenoviruses expressing CaM-WT or CaM mutants. We found that CaM-WT and a gain-of-function (GOF) CaM mutant (M37Q) promoted Ca^{2+} alternans and prolonged Ca^{2+} transient recovery, whereas a loss-of-function CaM mutation CaM (1–4) suppressed Ca^{2+} alternans and shortened Ca^{2+} transient recovery in both WT and RyR2 mutant hearts. Furthermore, we developed a novel numerical myocyte model for Ca^{2+} alternans, which incorporates the key feature of RyR2 inactivation by Ca^{2+}-CaM. Remarkably, our new model recapitulates the impact of RyR2 and CaM mutations on Ca^{2+} alternans. Our numerical simulations also reveal novel and important insights into the induction and progression of Ca^{2+} alternans.

METHODS

Data Availability

All data and supporting materials associated with this study are available in the article and the Data Supplement. The alternans analysis tool written in MATLAB and the simulation codes for the mathematical cell model are available upon request. Please contact R. Benitez (raul.benitez@upc.edu) for alternans analysis tool and B. Echebarria (blas.echebarria@upc.edu) for the simulation codes.

To assess the role of CaM in Ca^{2+} alternans in cardiac cells in the setting of intact working hearts and to avoid global detrimental impact of altered CaM function, we performed local adenovirus-mediated gene delivery in vivo by directly injecting adenoviruses expressing the CaM-WT, CaM (1–4), and CaM-M37Q mutants into the anterior wall of the left ventricle.[39] Five days after adenovirus injection, the hearts were isolated and Ca^{2+} transients were measured in Langendorff-perfused intact hearts loaded with Rhod-2 AM using laser scanning confocal Ca^{2+} imaging as described previously.[40,41] The recovery of voltage-induced Ca^{2+} transients was determined by using the S1S2 stimulation protocol as described previously with some modifications.[16,27,28] SR Ca^{2+} content was determined by measuring the amplitude of Ca^{2+} transients induced by local delivery of 20 mmol/L caffeine. The recovery from inactivation of the I_{Ca} was determined by using whole-cell patch-clamp recordings of isolated ventricular myocytes and the S1-S2 stimulation protocol as described previously.[38,42] The levels of adenovirus-mediated expression of CaM-WT and CaM mutants were determined by immunoblotting. Numerical simulations were performed using a modification of the Bondarenko model of a mouse ventricular myocyte.[43] Adult RyR2-R4496C$^{+/-}$ and RyR2-E4872Q$^{+/-}$ heterozygous mutant and WT control mice (8–16 weeks) were used for all experiments. Detailed methods are provided in the Data Supplement.

RESULTS

CaM Is an Important Determinant of Ca^{2+} Alternans in Intact Hearts

To assess the role of CaM in Ca^{2+} alternans, we determined the effect of altered CaM function on Ca^{2+} alternans. We used 2 CaM mutations: a loss-of-function CaM mutation, CaM (1–4) in which all 4 EF-hand Ca^{2+} binding sites are disabled, and a GOF CaM mutation, CaM-M37Q that enhances the CaM-dependent inhibition of RyR2-mediated spontaneous Ca^{2+} release.[44] To study Ca^{2+} alternans in the context of intact hearts and to minimize systemic adverse effect of CaM mutations, we infected mouse hearts in vivo by directly injecting adenoviruses harboring the CaM-WT, CaM (1–4), or CaM-M37Q mutant (Figure IA in the Data Supplement) into the anterior wall of the left ventricle.[39] We monitored Ca^{2+} transients in ventricular myocytes near the adenovirus-injection site in Langendorff-perfused intact hearts using confocal Ca^{2+} imaging. We also recorded Ca^{2+} transients in ventricular myocytes in the posterior wall of the left ventricle (away from the anterior injection

site), which serves as an internal control (Figure IB in the Data Supplement). As shown in Figure 1, Ca^{2+} alternans in intact hearts without adenovirus-injection (control) occurred at a stimulation frequency of ≈10 to 11 Hz (Figure 1A and 1E). This threshold frequency at which alternans occurs was decreased to ≈8 to 9 Hz in ventricular myocytes near the CaM-WT adenovirus-injection site in the anterior wall of the left ventricle (Figure 1B and 1E). The threshold frequency for Ca^{2+} alternans in ventricular myocytes near the CaM-M37Q injection site was substantially decreased to ≈7 Hz (Figure 1D and 1E). In contrast, the threshold frequency for Ca^{2+} alternans in ventricular myocytes near the CaM (1–4) injection site was markedly increased to ≈12 to 13 Hz (Figure 1C and 1E). However, there were no significant differences in the alternans ratios at 6 to 14 Hz in ventricular myocytes in the posterior wall of the left ventricle (away from the adenovirus-injection site) with or without infection with CaM-WT, CaM (1–4), or CaM-M37Q adenoviruses (Figure IC in the Data Supplement). Furthermore, immunoblotting analysis showed a significantly increased level of CaM expression after infection with CaM-WT, CaM (1–4), or CaM-M37Q adenoviruses in the anterior wall around the injection site, but an unchanged level of CaM expression in the posterior wall away from the injection site, compared with control (Figure IF and IG in the Data Supplement). Therefore, the adenovirus-injection mediated expression of CaM-WT, CaM-M37Q, and CaM (1–4) and their functional impact were confined to the area near the injection site.

To directly visualize the confined expression of locally injected CaM-WT or CaM mutant adenoviruses, we used adenoviruses coexpressing CaM-WT or CaM (1–4) together with the GFP (green fluorescence protein) marker (Figure 2A). We performed the same local in vivo gene delivery to the mouse hearts by directly injecting adenoviruses expressing CaM-WT/GFP or CaM (1–4)/GFP into the anterior wall of the left ventricle. As shown in Figure 2, the fluorescent GFP marker was detected only in the anterior wall around the injection site, but not in the posterior wall away from the injection site, nor in the control heart (Figure 2B). We also performed confocal Ca^{2+} imaging of intact hearts locally infected with or without the CaM-WT/GFP or CaM (1–4)/GFP adenoviruses to assess their impact on Ca^{2+} alternans (Figure 2C). As with CaM-WT and CaM (1–4) adenoviruses, we found that CaM-WT/GFP decreased the threshold frequency at which alternans occurs to ≈8 to 9 Hz (from ≈10 to 11 Hz in control), whereas CaM (1–4)/GFP increased the alternans threshold frequency to ≈12 to 13 Hz (Figure IIA through IID in the Data Supplement). There were no significant differences in the alternans ratios at all stimulation frequencies (6–14 Hz) between CaM-WT and CaM-WT/GFP or between CaM (1–4) and CaM (1–4)/GFP adenovirus infected intact hearts (Figure IIIA in the Data Supplement). Furthermore, expression of CaM-WT/GFP or CaM (1–4)/GFP did not significantly affect the amplitude, time-to-peak, or decay time (at 50% or 90%) of Ca^{2+} transients compared with control (Figure IV in the Data Supplement). Immunoblotting analysis also showed a significantly increased level of CaM expression after infection with CaM-WT/GFP or CaM (1–4)/GFP adenoviruses in the anterior wall around the injection site, but an unchanged level of CaM expression in the posterior wall away from the injection site compared with control (Figure 2D and 2E). Taken together, these observations indicate that enhancing CaM function (as in the GOF CaM mutation M37Q) promotes Ca^{2+} alternans, whereas suppressed CaM function (as in the loss-of-function CaM mutation CaM [1–4]) diminished it. Therefore, CaM is an important determinant of pacing-induced Ca^{2+} alternans in intact hearts.

CaM Regulates the Recovery of Depolarization-Induced Ca^{2+} Transients in Intact Hearts

Ca^{2+} alternans is thought to result from beat-to-beat alternations in the refractoriness of depolarization-induced Ca^{2+} transients.[16,23,27,29,30] Thus, CaM may affect Ca^{2+} alternans by modulating Ca^{2+} transient refractoriness. To test this, we assessed the effect of CaM-WT, CaM (1–4), or CaM-M37Q on the recovery of depolarization-induced Ca^{2+} transients in intact hearts. The recovery of Ca^{2+} transients in ventricular myocytes near or away from the adenovirus-injection sites was determined using the S1S2 stimulation protocol[16] in isolated Langendorff-perfused intact hearts. As shown in Figure 1, the recovery of the Ca^{2+} transient amplitude at various S1S2 intervals (≈60–160 ms) was slightly (but not significantly) prolonged in ventricular myocytes near the CaM-WT adenovirus-injection site in the anterior wall of the left ventricle (Figure 1G, 1J, and 1K) and was markedly prolonged in cells near the CaM-M37Q injection site (Figure 1I through 1K), compared with that in ventricular myocytes without infection (control; Figure 1F, 1J, and 1K). However, the recovery of the Ca^{2+} transient amplitude in ventricular myocytes near the CaM (1–4) adenovirus-injection site was substantially accelerated (Figure 1H, 1J, and 1K). There are no significant differences in the recovery of the Ca^{2+} transient amplitudes in ventricular myocytes in the posterior wall of the left ventricle (away from the adenovirus-injection site) with or without infection with CaM-WT, CaM (1–4), or CaM-M37Q adenoviruses (Figure ID in the Data Supplement). Furthermore, the recovery of the Ca^{2+} transient amplitude at various S1S2 intervals (≈75–125 ms) was slightly and significantly prolonged in ventricular myocytes near the CaM-WT/GFP adenovirus-injection site in the anterior wall of the left ventricle compared with that in ventricular myocytes without infection (control; Figure IIE through III). In contrast, the recovery of the Ca^{2+} transient amplitude in ventricular myocytes near the CaM (1–4)/GFP

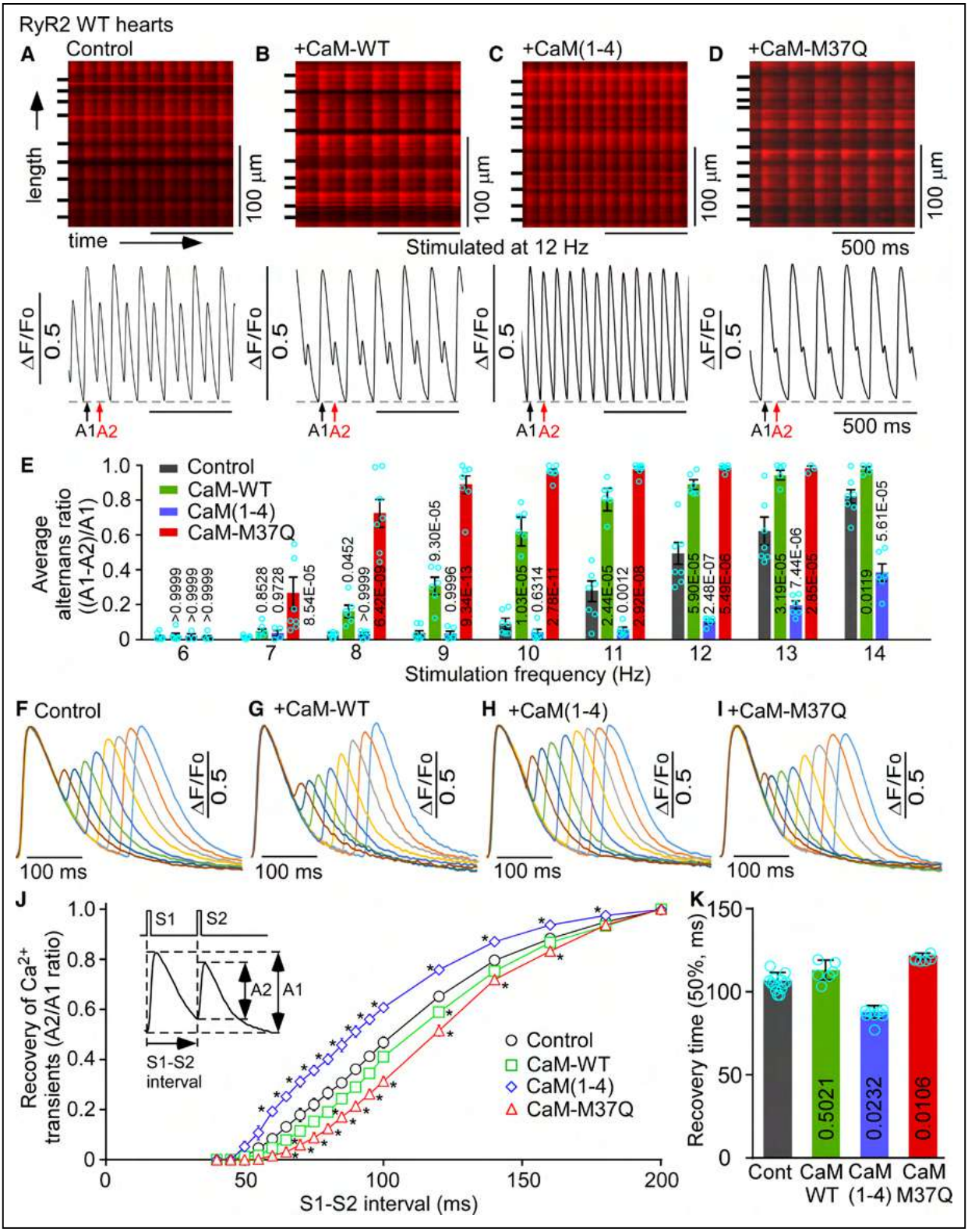

Figure 1. Effects of altered CaM (calmodulin) function on Ca^{2+} alternans and Ca^{2+} transient recovery in intact RyR2 (ryanodine receptor 2) wild-type (WT) hearts.

RyR2 WT hearts without injection (**A**, control) or locally injected with adenoviruses expressing CaM-WT (**B**), CaM (1–4) (**C**), or CaM-M37Q (**D**) were loaded with Rhod-2 AM. Ca^{2+} transients in intact Rhod-2 AM loaded hearts were elicited by pacing at different frequencies (6–14 Hz) and recorded using line-scanning confocal imaging. Cell boundaries were indicated by short bars to the **left**. The ΔF/Fo traces depict the average fluorescence signal of the scan area. **E**, Alternans ratios for each cell that displayed alternans in the scan area were determined and averaged per cell to yield the average alternans ratio. Alternans ratio is defined as the ratio of the difference in amplitude (*Continued*)

adenovirus-injection site was substantially accelerated compared with control (Figure IIE through III in the Data Supplement). There were no significant differences in the recovery of the Ca^{2+} transient amplitude at all S1S2 intervals (≈50–200 ms) between CaM-WT and CaM-WT/GFP or between CaM (1–4) and CaM (1–4)/GFP adenovirus infected intact hearts (Figure IIIB in the Data Supplement). Collectively, these observations indicate that the GOF CaM-M37Q mutation prolongs the recovery of Ca^{2+} transients, whereas the loss-of-function CaM (1–4) mutation shortens it. Thus, CaM has an important role in determining the recovery of Ca^{2+} transients.

Effects of CaM-WT and the CaM (1–4) Mutant on SR Ca^{2+} Content and the Recovery From Inactivation of the I_{Ca}

SR Ca^{2+} content is one of the key determinants of Ca^{2+} transient amplitude. To assess whether the effects of altered CaM function on Ca^{2+} transient alternans are secondary to CaM-dependent changes in SR Ca^{2+} content, we measured SR Ca^{2+} content in GFP-expressing ventricular myocytes isolated from tissues near the CaM-WT/GFP or CaM (1–4)/GFP adenovirus-injection site in the anterior wall of the left ventricle. Single-cell Ca^{2+} imaging showed that CaM-WT/GFP- and CaM (1–4)/GFP-expressing ventricular myocytes displayed amplitude of caffeine (20 mmol/L) induced Ca^{2+} release similar to that of control cells (Figure 3A through 3D). Note that the level of fluorescence signals evoked by 20 mmol/L caffeine was not saturated as a much higher level of fluorescence signals could still be detected under the same conditions.[28] Thus, adenovirus-mediated expression of CaM-WT or CaM (1–4) does not significantly alter the SR Ca^{2+} content in ventricular myocytes under our experimental conditions.

In ventricular myocytes, the I_{Ca} triggers Ca^{2+} transients. Thus, it is possible that the recovery from inactivation of the I_{Ca} would affect the recovery of Ca^{2+} transients. To test this possibility, we assessed and compared the recovery of the Ca^{2+} transient amplitude and the recovery from inactivation of the I_{Ca} in isolated CaM-WT/GFP- and CaM (1–4)/GFP-expressing ventricular myocytes and control cells using confocal Ca^{2+} imaging and whole-cell patch-clamp recordings, respectively. CaM-WT significantly prolonged the recovery of the Ca^{2+} transient amplitude with an average 50% recovery time of ≈270 ms, compared with control (≈220 ms). In contrast, CaM (1–4) significantly accelerated the recovery of the Ca^{2+} transient amplitude with an average 50% recovery time of ≈140 ms (Figure 3E through 3I). As with the recovery of the Ca^{2+} transient amplitude, CaM-WT significantly prolonged the recovery from inactivation of the I_{Ca} with an average 50% recovery time of ≈85ms compared with control (≈60 ms), whereas CaM (1–4) significantly accelerated it with an average 50% recovery time of ≈40 ms (Figure 3J through 3N). However, the 50% recovery time from inactivation of the I_{Ca} is markedly shorter than the 50% recovery time of the Ca^{2+} transient amplitude in the control, CaM-WT or CaM (1–4) expressing cells, respectively. In other words, there is little or no recovery of Ca^{2+} transients from inactivation when the I_{Ca} has already recovered to 50%. This implies that although the recovery from inactivation of the I_{Ca} can influence the recovery of Ca^{2+} transient amplitude, it is unlikely to be the rate-limiting factor. Furthermore, CaM-WT or mutant did not significantly alter the peak I_{Ca} (Figure IIID in the Data Supplement), similar to those reported previously.[38,45] These observations suggest that other factors, for instance, the recovery from inactivation of the RyR2 channel may play a critical role in determining the recovery of the Ca^{2+} transient amplitude. Consistent with this view, experimental and numerical modeling studies also suggest that the recovery of RyR2 from inactivation significantly contributes to the induction of Ca^{2+} transient alternans.[16,20,23,27,29,30,33]

Effects of CaM mutations on Ca^{2+} Alternans and Ca^{2+} Transient Recovery in Intact RyR2-E4872Q Hearts

We have previously shown that the RyR2-E4872Q mutation abolishes luminal Ca^{2+} activation of RyR2 and markedly promotes Ca^{2+} alternans.[27,28] Thus, both CaM- and luminal Ca^{2+}-dependent regulation of RyR2 play an important role in Ca^{2+} alternans. To determine whether there is a cross-talk between the CaM- and luminal Ca^{2+}-dependent regulatory mechanisms of Ca^{2+} alternans, we assessed the effect of altered CaM function on Ca^{2+} alternans in intact RyR2-E4872Q mutant hearts. As shown in Figure 4, Ca^{2+} alternans in intact RyR2-E4872Q mutant hearts without injection (control)

Figure 1 Continued. between the large and small Ca^{2+} transients over the amplitude of the large Ca^{2+} transient. Data are mean±SEM (n=7 hearts for control, 6 hearts for CaM-WT, 6 hearts for CaM [1–4], and 7 hearts for CaM-M37Q with their *P* values indicated for each condition vs control). To determine the recovery of Ca^{2+} transients, control (**F**), CaM-WT (**G**), CaM (1–4) (**H**), or CaM-M37Q (**I**) adenovirus-injected hearts were first stimulated at 5 Hz for 30 beats (S1), followed by a single S2 stimulation. A series of S1S2 stimulations were repeatedly applied with progressively reduced S1S2 intervals from 200 to 40 ms. Ca^{2+} transients were recorded using line-scanning confocal imaging. **J**, The relationship between A2/A1 ratio of the Ca^{2+} transient amplitude and the S1S2 interval (*$P<0.05$ vs control). **K**, The 50% recovery time of the Ca^{2+} transient amplitude after pacing with the S1S2 protocol. Data are mean±SEM (n=13 hearts for control, 6 hearts for CaM-WT, 8 hearts for CaM [1–4], and 6 hearts for CaM-M37Q with their *P* values indicated for each condition vs control; 2-way ANOVA with Dunnett post hoc test for obtaining the adjusted *P* values shown in **E** and **J**, and Kruskal-Wallis test with Dunn post hoc test for obtaining the adjusted *P* values shown in **K**, all conditions vs control).

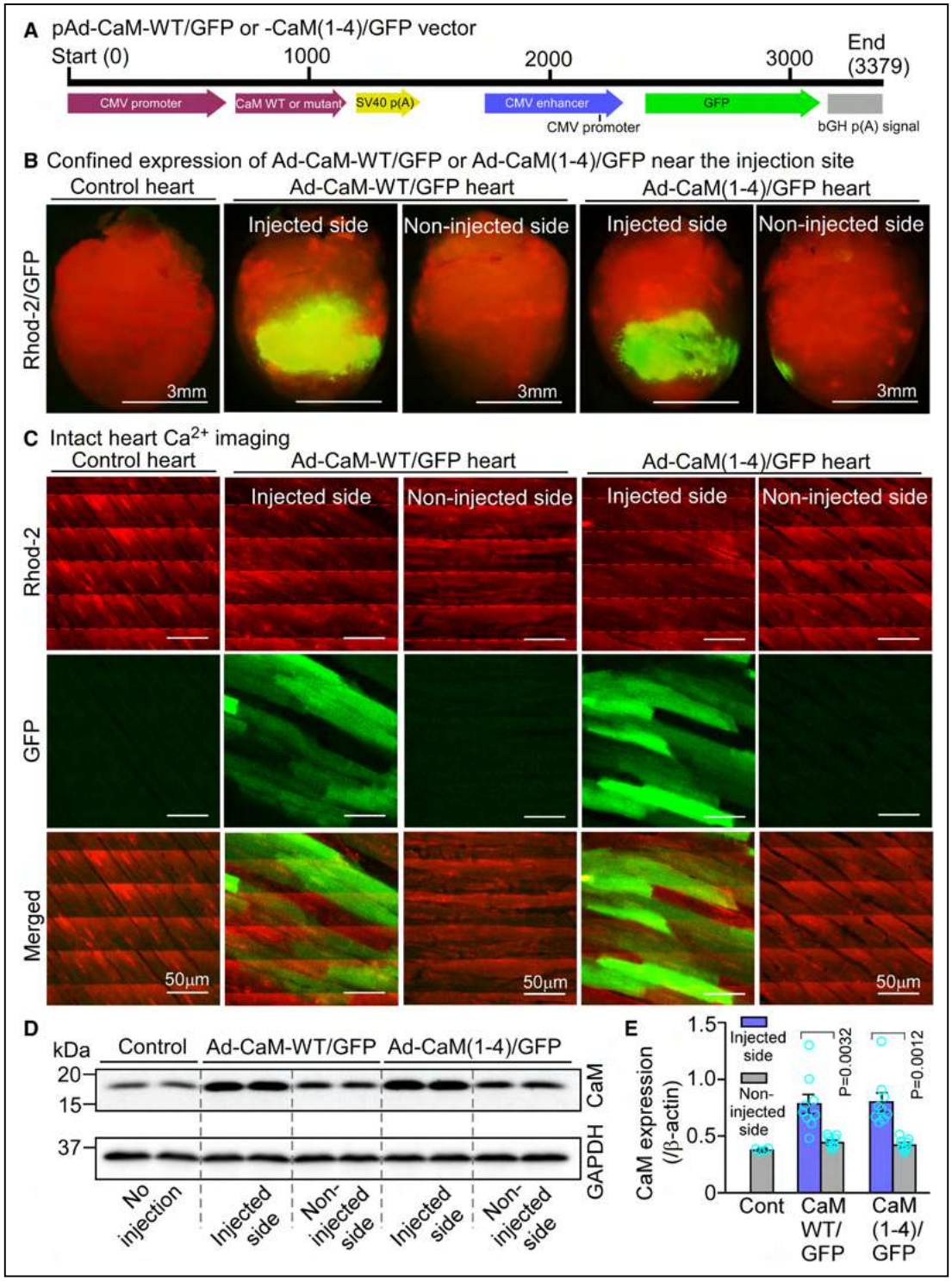

Figure 2. Local expression of CaM (calmodulin)-wild-type (WT)/GFP (green fluorescence protein) and CaM (1–4)/GFP in intact hearts after in vivo adenovirus-mediated gene delivery.

A, A schematic diagram of plasmids used to produce the adeno-associated viruses (AAV) coexpressing CaM-WT/GFP or CaM (1–4)/GFP. **B**, Merged Rhod-2 (red) and GFP (green) fluorescent images of control hearts, hearts injected with Ad-CaM-WT/GFP (injected side vs noninjected side), and hearts injected with Ad-CaM (1–4)/GFP (injected side vs noninjected side), showing locally confined expression of Ad-CaM-WT/GFP or Ad-CaM (1–4)/GFP near the injection site. Scale bars, 3 mm. **C**, Confocal line-scan *x-y* Rhod-2, GFP, or merged images of control hearts or hearts injected with Ad-CaM-WT/GFP or Ad-CaM (1–4)/GFP (injected side vs noninjected side) paced at 5 Hz. Red dash-lines indicate Ca^{2+} transients. Scale bars, 50 μm. **D**, Immunoblotting of tissues isolated from the anterior wall of the left ventricle of control hearts (no injection) or from the left ventricular anterior wall around the sites of injection (injected sites) of CaM-WT/GFP or CaM (1–4)/GFP adenoviruses or from the posterior wall (away from the injection sites, noninjected sites) of the left ventricle. **E**, Quantification of CaM expression 5 d post adenoviral injection. Data are mean±SEM (n=4 hearts for control, 9 hearts for CaM-WT/GFP, and 8 hearts for CaM [1–4]/GFP; paired Student *t* test, injected side vs noninjected site).

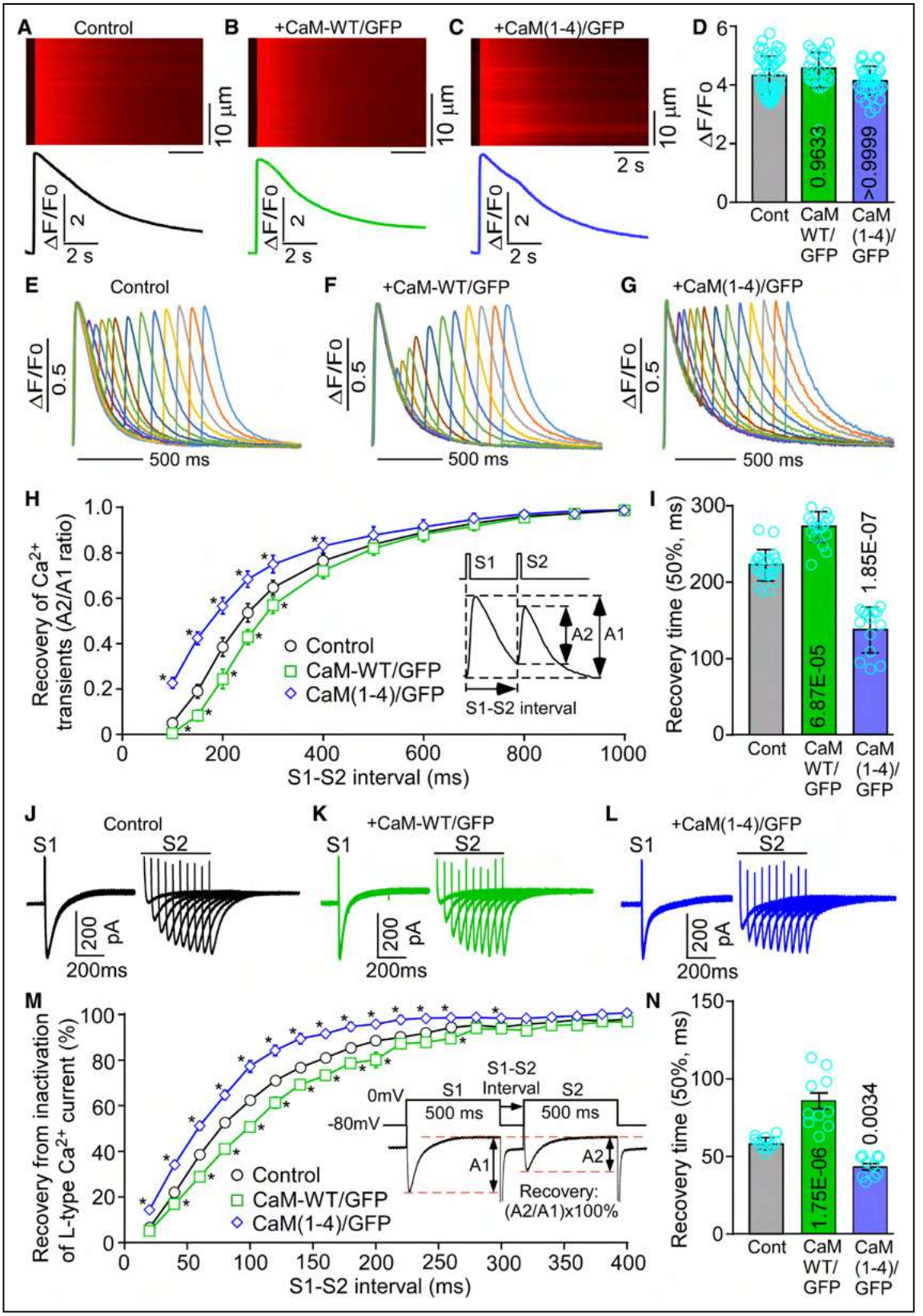

Figure 3. Effects of altered CaM (calmodulin) function on sarcoplasmic reticulum (SR) Ca^{2+} content, recovery of Ca^{2+} transients, and recovery from inactivation of L-type Ca^{2+} current.

SR Ca^{2+} contents in Rhod-2 AM loaded mouse ventricular myocytes isolated from RyR2 (ryanodine receptor 2) wild-type (WT) hearts without injection (control; **A**), or from WT hearts locally injected with Ad-CaM-WT/GFP (green fluorescence protein; **B**) or Ad-CaM (1–4)/GFP (**C**) were determined by measuring the amplitude of caffeine (20 mmol/L)-induced Ca^{2+} release (**D**). (*Continued*)

occurred at a stimulation frequency of ≈8 Hz (Figure 4A and 4D), which is significantly lower than that (≈11 Hz) in intact WT hearts (Figure 1). As with WT hearts, CaM (1–4) increased the threshold frequency for Ca^{2+} alternans from ≈8 Hz to ≈10 Hz in ventricular myocytes near the injection site in the anterior wall of the left ventricle of the RyR2-E4872Q hearts (Figure 4B and 4D), whereas CaM-M37Q decreased the threshold frequency for Ca^{2+} alternans from ≈8 to ≈5 to 6 Hz (Figure 4C and 4D). However, there are no significant differences in alternans ratios at 5 to 12 Hz in ventricular myocytes in the posterior wall of the left ventricle (away from the injection site) of intact RyR2-E4872Q hearts with or without infection with CaM (1–4) or CaM-M37Q (Figure VB in the Data Supplement).

We also assessed the effect of altered CaM function on the recovery of Ca^{2+} transients in intact RyR2-E4872Q mutant hearts. CaM (1–4) accelerated the recovery of depolarization-induced Ca^{2+} transient amplitude (Figure 4F, 4H, and 4I), whereas CaM-M37Q delayed the recovery of the Ca^{2+} transient amplitude in intact RyR2-E4872Q mutant hearts (Figure 4G, 4H, and 4I), compared with control (Figure 4E, 4H, and 4I). There are no significant differences in the recovery of the Ca^{2+} transient amplitude in ventricular myocytes in the posterior wall of the left ventricle (away from the adenovirus-injection site; Figure VB and VC in the Data Supplement). Thus, CaM can still modulate the Ca^{2+} transient recovery and Ca^{2+} alternans in intact RyR2-E4872Q hearts with diminished luminal Ca^{2+} regulation of RyR2.

Effects of CaM Mutations on Ca^{2+} Alternans and Ca^{2+} Transient Recovery in Intact RyR2-R4496C Hearts

We have also shown previously that the RyR2-R4496C mutation enhances luminal Ca^{2+} activation of RyR2 and dramatically suppresses Ca^{2+} alternans.[28] To further investigate the cross-talk between the CaM- and luminal Ca^{2+}-dependent regulatory mechanisms of Ca^{2+} alternans, we assessed the effect of altered CaM function on Ca^{2+} alternans in intact RyR2-R4496C mutant hearts. As shown in Figure 5, Ca^{2+} alternans in intact RyR2-R4496C hearts without injection occurred at a stimulation frequency of ≈13 to 14 Hz (Figure 5A and 5D), which is significantly higher than that (≈11 Hz) in intact WT hearts (Figure 1). CaM (1–4) increased the threshold frequency for Ca^{2+} alternans from ≈13 to 14 to ≈15 Hz in ventricular myocytes near the injection site in the anterior wall of the left ventricle of the RyR2-R4496C hearts (Figure 5B and 5D), whereas CaM-M37Q decreased the threshold frequency for Ca^{2+} alternans from ≈13 to 14 to ≈8 to 9 Hz (Figure 5C and 5D). Similarly, there are no significant differences in alternans ratios at 8 to 15 Hz in ventricular myocytes in the posterior wall of the left ventricle (away from the injection site) of intact RyR2-R4496C hearts with or without infection with CaM (1–4) or CaM-M37Q (Figure VD in the Data Supplement).

CaM (1–4) also accelerated the recovery of the Ca^{2+} transient amplitude (Figure 5F, 5H, and 5I), whereas CaM-M37Q delayed the recovery of the Ca^{2+} transient amplitude in intact RyR2-R4496C mutant hearts (Figure 5G, 5H, and 5I), compared with control (Figure 5E, 5H, and 5I). There are no significant differences in the recovery of the Ca^{2+} transient amplitude in ventricular myocytes in the posterior wall of the left ventricle (away from the injection site) of intact RyR2-R4496C hearts with or without infection with CaM (1–4) or CaM-M37Q (Figure VE and VF in the Data Supplement). Taken together, enhanced CaM function promotes, whereas decreased CaM function suppresses Ca^{2+} alternans. In contrast, enhanced RyR2 luminal Ca^{2+} activation suppresses, whereas decreased RyR2 luminal Ca^{2+} activation promotes Ca^{2+} alternans. Thus, CaM and RyR2 luminal Ca^{2+} activation regulate Ca^{2+} transient recovery and Ca^{2+} alternans in a counter-balanced manner.

A Novel Numerical Model Recapitulates the Action of CaM in Ca^{2+} Alternans in Intact WT Hearts

Previous numerical simulations have shown that RyR2 inactivation plays a key role in the induction of Ca^{2+} alternans.[20,33] However, the molecular basis for RyR2

Figure 3 Continued. Data are mean±SEM (n=47 cells from 10 hearts for control, 28 cells, 5 hearts for CaM-WT/GFP, and 34 cells, 6 hearts for CaM [1–4]/GFP with their *P* values indicated for each condition vs control). To determine the recovery of Ca^{2+} transients, control (**E**), CaM-WT/GFP (**F**), or CaM (1–4)/GFP (**G**) expressing ventricular myocytes were first stimulated at 1 Hz for 10 beats (S1), followed by a single S2 stimulation. A series of S1S2 stimulations were repeatedly applied with progressively reduced S1S2 intervals from 1000 to 100 ms. Ca^{2+} transients were recorded using line-scanning confocal imaging. **H**, The relationship between A2/A1 ratio of the Ca^{2+} transient amplitude and S1S2 interval. **I**, The 50% recovery time of the Ca^{2+} transient amplitude after pacing with the S1S2 protocol. Data are mean±SEM (n=24 cells from 8 hearts for control, 15 cells, 6 hearts for CaM-WT/GFP, and 14 cells, 5 hearts for CaM [1–4]/GFP with their *P* values indicated for each condition vs control). To assess the recovery from inactivation of the L-type Ca^{2+} current, ventricular myocytes isolated from control hearts (**J**), CaM-WT/GFP (**K**), or CaM (1–4)/GFP (**L**) adenovirus-injected hearts were first stimulated at 1 Hz for 5 beats (S1), followed by a single S2 stimulation. A series of S1S2 stimulations were repeatedly applied with progressively increased S1S2 intervals from 20 to 400 ms. L-type Ca^{2+} currents were recorded using whole-cell patch-clamp recording. **M**, The relationship between A2/A1 ratio of the L-type Ca^{2+} current amplitude and the S1S2 interval (*$P<0.05$ vs control). **N**, The 50% recovery time of L-type Ca^{2+} current for control, CaM-WT/GFP, or CaM (1–4)/GFP-expressing cells. Data are mean±SEM (n=12 cells from 5 hearts for control, 10 cells from 5 hearts for CaM-WT/GFP, 10 cells from 5 hearts for CaM [1–4]/GFP with their *P* values indicated for each condition vs control; values of SEM were adjusted with the hierarchical statistical method,[64] 1-way ANOVA with Bonferroni post hoc test for obtaining the adjusted *P* values shown in **D, H**, **I**, **M**, and **N**, all conditions vs control).

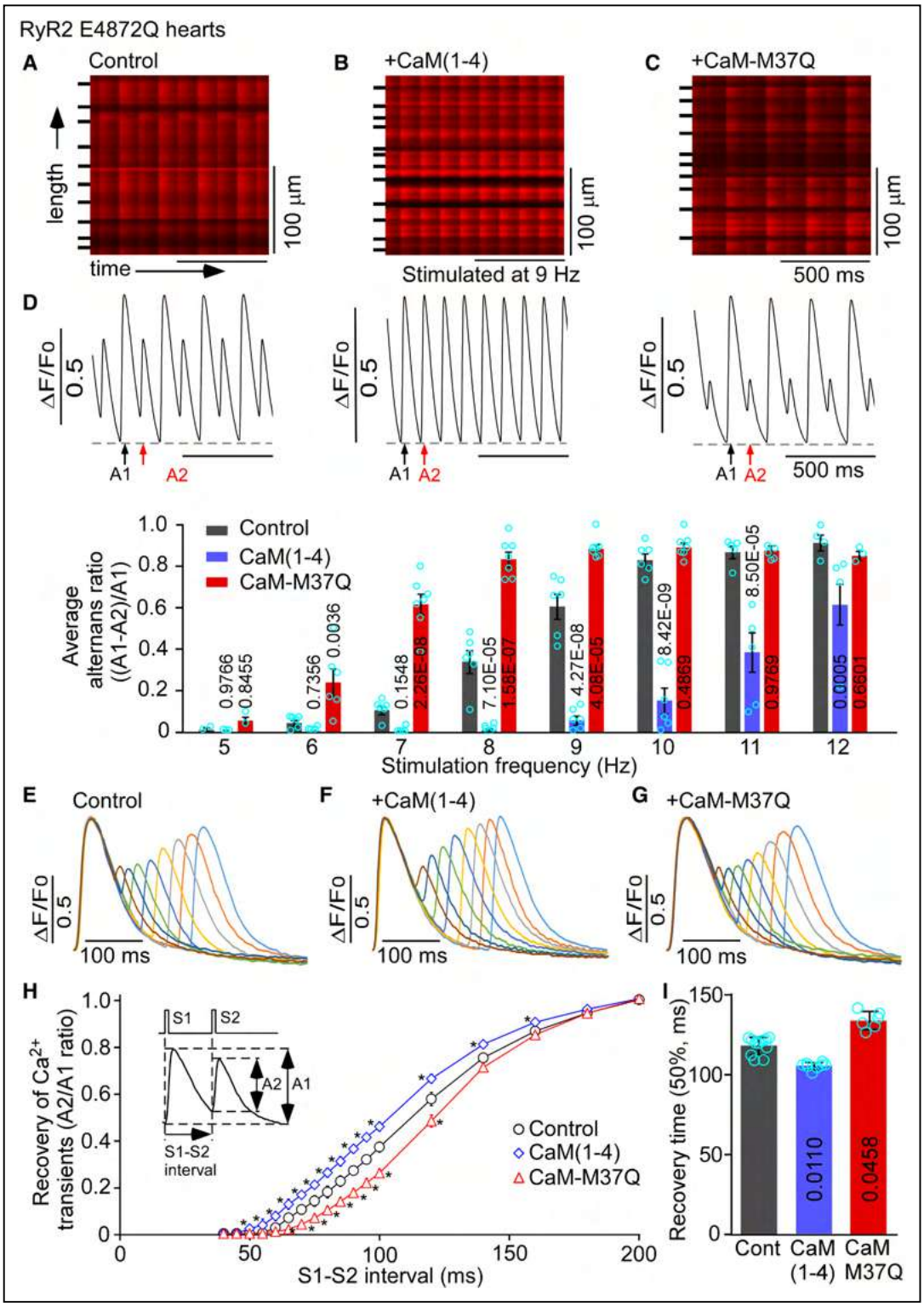

Figure 4. Effects of CaM (calmodulin) mutations on Ca^{2+} alternans and Ca^{2+} transient recovery in intact RyR2 (ryanodine receptor 2)-E4872Q mutant hearts.

RyR2-E4872Q mutant hearts without injection (**A**, control) and with local injection of CaM (1–4) (**B**) or CaM-M37Q (**C**) adenoviruses were stimulated at increasing frequencies (5–12 Hz). **D**, Alternans ratios. Data are mean±SEM (n=6 hearts for control, 6 hearts for CaM [1–4], and 7 hearts for CaM-M37Q with their *P* values indicated for each condition vs control). Recovery of Ca^{2+} transients in control (**E**), CaM (1–4) (**F**), or CaM-M37Q (**G**) hearts. **H**, The relationship between A2/A1 ratio of the Ca^{2+} transient amplitude and the S1S2 interval (*P<0.05 vs control). **I**, The 50% recovery time of the Ca^{2+} transient amplitude after pacing with the S1S2 protocol. Data are mean±SEM (n=11 hearts for control, 8 hearts for CaM [1–4], and 6 hearts for CaM-M37Q with their *P* values indicated for each condition vs control; 2-way ANOVA with Dunnett post hoc test for obtaining the adjusted *P* values shown in **D** and **H**, Kruskal-Wallis test with Dunn post hoc test for obtaining the adjusted *P* values shown in **I**, all conditions vs control).

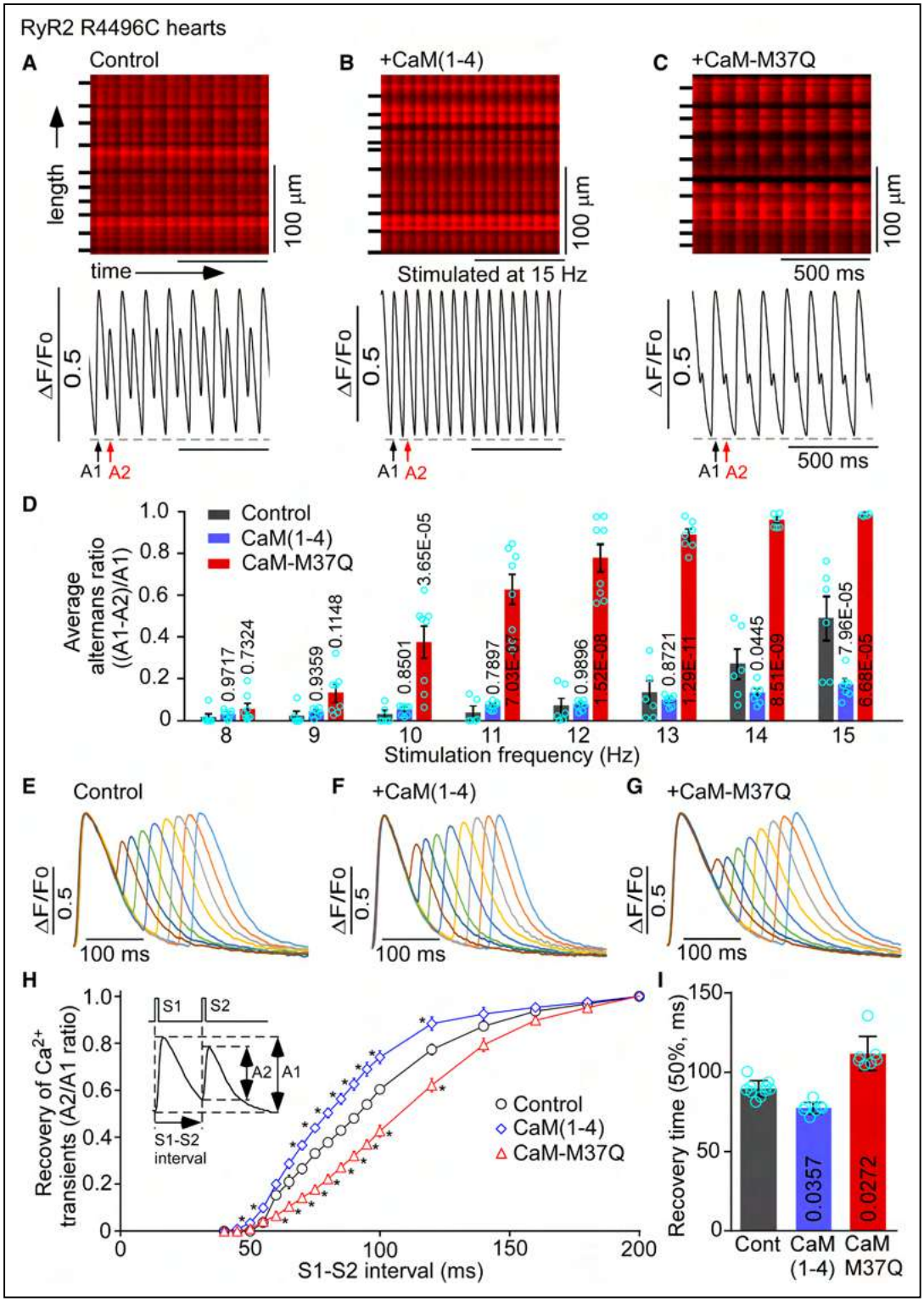

Figure 5. Effects of CaM (calmodulin) mutations on Ca^{2+} alternans and Ca^{2+} transient recovery in intact RyR2 (ryanodine receptor 2)-R4496C mutant hearts.

RyR2-R4496C mutant hearts without injection (**A**, control) and with local injection of CaM (1–4) (**B**) or CaM-M37Q (**C**) adenoviruses were stimulated at increasing frequencies (8–15 Hz). **D**, Alternans ratios. Data are mean±S.E.M (n=6 hearts for control, 7 hearts for CaM [1–4], and 8 hearts for CaM-M37Q with their *P* values indicated for each condition vs control). Recovery of Ca^{2+} transients in control (**E**), CaM (1–4) (**F**), or CaM-M37Q (**G**) hearts. **H**, The relationship between A2/A1 ratio of the Ca^{2+} transient amplitude and the S1S2 interval (*P<0.05 vs control). **I**, The 50% recovery time of the Ca^{2+} transient amplitude after pacing with the S1S2 protocol. Data are mean±SEM (n=10 hearts for control, 7 hearts for CaM (1–4), and 7 hearts for CaM-M37Q with their *P* values indicated for each condition vs control; 2-way ANOVA with Dunnett post hoc test for obtaining the adjusted *P* values shown in **D** and **H**, Kruskal-Wallis test with Dunn post hoc test for obtaining the adjusted *P* values shown in **I**, all conditions vs control).

inactivation and the induction of Ca^{2+} alternans is unknown. Given the involvement of CaM in the inactivation of RyR2, the termination and refractoriness of Ca^{2+} release,[34,37,38] and Ca^{2+} alternans (Figures 1 through 5), we developed a numerical model of Ca^{2+} alternans by incorporating the Ca^{2+}-CaM-dependent inactivation of RyR2 and recovery of RyR2 from this inactivation into the Bondarenko model of mouse ventricular myocytes[43] (Figure 6A and 6B; Figure VI in the Data Supplement). The L-type Ca^{2+} channel is also known to be modulated by CaM.[46] Hence, we incorporated the Ca^{2+}-CaM dependent regulation of L-type Ca^{2+} channel as well. Furthermore, since SR luminal Ca^{2+} activation of RyR2 is important for the induction of Ca^{2+} alternans,[27,28] we also included the highly steep activation of RyR2 by SR luminal Ca^{2+} into the modified model (Figure 6A and 6B; Figure VI in the Data Supplement). In addition, we modified the binding of Ca^{2+} to CaM, added the Rhod-2 dye, and included mitochondria Ca^{2+} handling in the model. Remarkably, this new model recapitulates the induction and progression of pacing-induced Ca^{2+} alternans in intact WT hearts (Figure 6C). The alternans ratios in RyR2-WT hearts at different pacing frequencies predicted by the model matched very closely those observed experimentally (Figure 6C and 6G).

To model the impact of altered CaM function on Ca^{2+} alternans, we modified the level and the affinity of Ca^{2+} binding to CaM to simulate the functional impact of CaM-WT, CaM (1–4), and CaM-M37Q (Materials in the Data Supplement). Importantly, our model also reproduced the effects of CaM-WT (Figure 6D), CaM (1–4; Figure 6E), and CaM-M37Q (Figure 6F) on Ca^{2+} alternans at different pacing frequencies in intact RyR2 WT hearts (Figure 6G). Therefore, our numerical model recapitulates not only the induction and progression of pacing-induced Ca^{2+} alternans in intact hearts but also the impact of CaM-WT and mutants on Ca^{2+} alternans.

Numerical Simulation Reproduces the Effects of RyR2 and CaM Mutations on Ca^{2+} Alternans in Intact RyR2-E4872Q and RyR2-R4496C Mutant Hearts

The RyR2-E4872Q mutation diminishes luminal Ca^{2+} activation and suppresses cytosolic Ca^{2+} activation of single RyR2 channels. E4872Q also increases the L-type Ca^{2+} channel current to maintain the amplitude of Ca^{2+} transients as a compensatory response to reduced SR Ca^{2+} release.[47] However, the RyR2-R4496C mutation enhances the luminal Ca^{2+} activation but has little effect on the cytosolic Ca^{2+} activation of single RyR2 channels.[48] To determine whether our numerical model is also able to reproduce the effect of altered RyR2 function on Ca^{2+} alternans, we modified in the model the response of RyR2 to cytosolic and luminal Ca^{2+} activation to incorporate the functional impact of the RyR2-E4872Q or RyR2-R4496C mutation. As shown in Figure 7, the alternans ratios at different pacing frequencies predicted by the model are remarkably similar to those obtained experimentally (Figure 7A, 7E, 7D, and 7H). More importantly, the model also recapitulated the actions of CaM (1–4) and CaM-M37Q mutations in Ca^{2+} alternans in the RyR2-E4872Q (Figure 7B, 7C, and 7D) and RyR2-R4496C (Figure 7F, 7G, and 7H) mutant hearts without implanting additional modifications to the model. Thus, the model is able to reproduce not only the effect of altered CaM function but also the effect of altered RyR2 function on Ca^{2+} alternans in intact hearts. Taken together, our numerical model recapitulates the induction and progression of Ca^{2+} alternans in intact hearts under 9 different experimental conditions.

CaM Is Critical for RyR2 Inactivation and Ca^{2+} Alternans

We next used the newly developed, experimentally validated numerical model to explore the mechanism of Ca^{2+} alternans. We first assessed the role of CaM in the inactivation of RyR2 and the occurrence of Ca^{2+} alternans. We analyzed the fraction of inactivated RyR2 and cytosolic Ca^{2+} transients at a stimulation frequency of 12 Hz before and after removing CaM (ie, setting the concentration of CaM to 0). As shown in Figure VII in the Data Supplement, removal of CaM from the system completely abolished RyR2 inactivation and Ca^{2+} alternans (Figure VIIA and VIIB in the Data Supplement). Thus, consistent with previous studies,[20,33] RyR2 inactivation and more specifically, Ca^{2+}-CaM-dependent RyR2 inactivation is a critical determinant of Ca^{2+} alternans.

Pacing-Induced Diastolic Cytosolic Ca^{2+} Elevation Triggers Ca^{2+}-CaM Dependent RyR2 Inactivation and Provokes Diastolic Cytosolic Ca^{2+} and RyR2 Inactivation Alternans

What then triggers Ca^{2+}-CaM-dependent inactivation of RyR2 and how does Ca^{2+}-CaM dependent RyR2 inactivation lead to Ca^{2+} alternans? To address these questions, we simulated the induction and progression of pacing-induced Ca^{2+} alternans using an S1S2 stimulation protocol with a basal stimulation (S1) at a given frequency (eg, at the alternans threshold frequency, 10.6 Hz, as described in Materials in the Data Supplement) followed by a second stimulation (S2) at various frequencies (eg, 12 Hz; Figure 8A). We analyzed the levels of diastolic cytosolic Ca^{2+} and diastolic fraction of Ca^{2+}-CaM inactivated RyR2 in the steady state at various S2 stimulation frequencies (9–12 Hz) after switching from 10.6 Hz (S1; Figure 8B through 8D). We focused on the diastolic fraction of inactivated RyR2 because it determines the

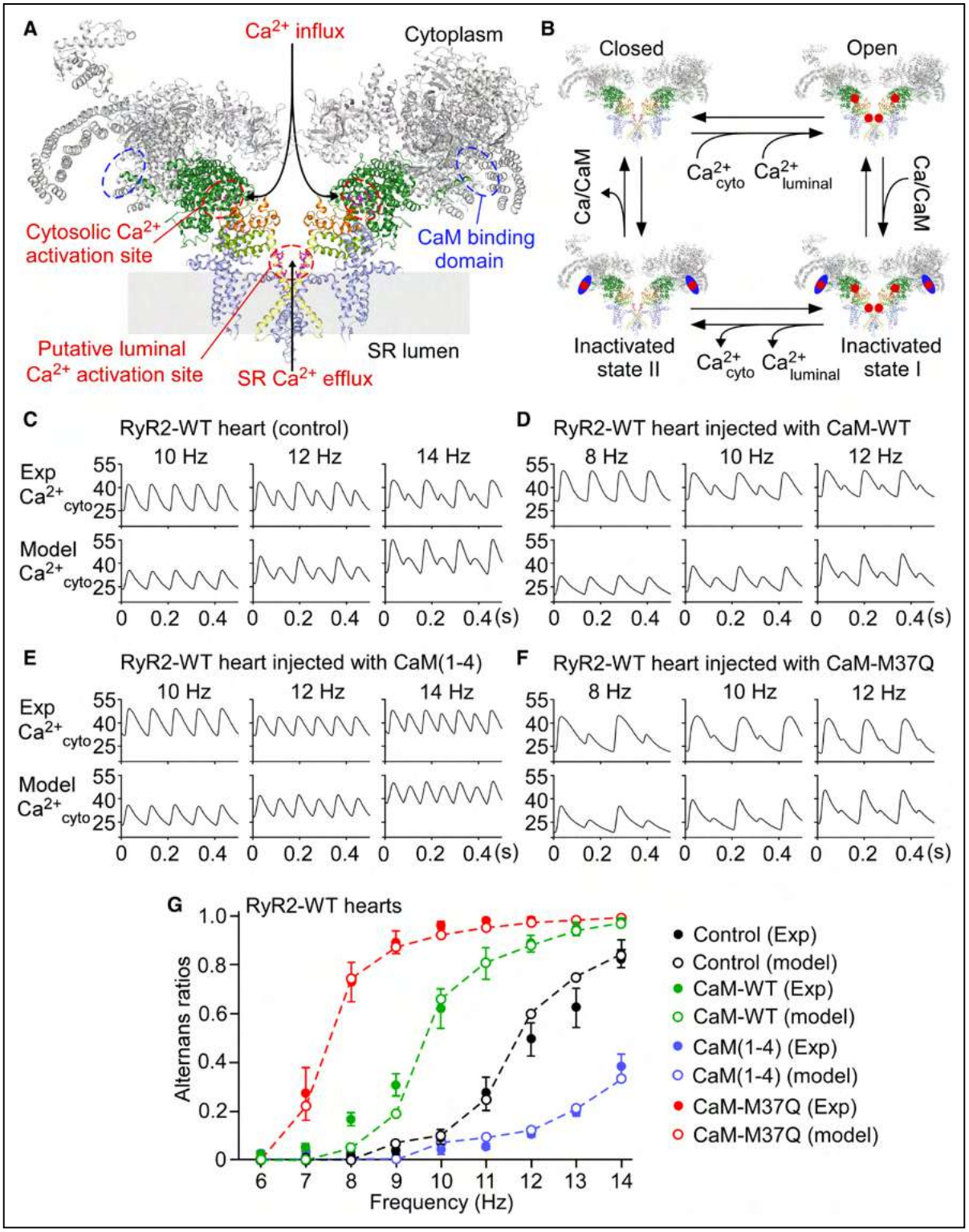

Figure 6. Numerical simulation of altered CaM (calmodulin) function on Ca^{2+} alternans in RyR2 (ryanodine receptor 2) wild-type (WT) hearts.

A, The 3-dimensional structure of RyR2[36] showing the locations of the cytosolic Ca^{2+} activation sites, the CaM binding site, and the putative luminal Ca^{2+} activation sites. For clarity, only 2 RyR2 subunits are shown. **B**, The 4-state model of RyR2. The RyR2 presents Ca^{2+} binding domains to both cytosolic and luminal Ca^{2+}, that activate the channel, and to CaM, that inactivates it. Inactivation of the RyR2 occurs as Ca^{2+} binds to CaM at the CaM binding site of the RyR2. There is a second inactivated state that corresponds to a RyR2 with Ca^{2+} bound to the CaM binding site but not to the cytosolic and luminal activation sites (Materials in the Data Supplement). The model was paced at several stimulation frequencies, obtaining a very good agreement with the experimental traces (**C**). The same procedure was followed for cells injected with CaM-WT (**D**), loss-of-function (LOF) CaM mutation CaM (1–4) (**E**), and gain-of-function (GOF) CaM mutant (M37Q; **F**). **G**, Comparison of the numerically obtained amplitude of alternans in the 4 cases with the experimental results, showing a very good agreement.

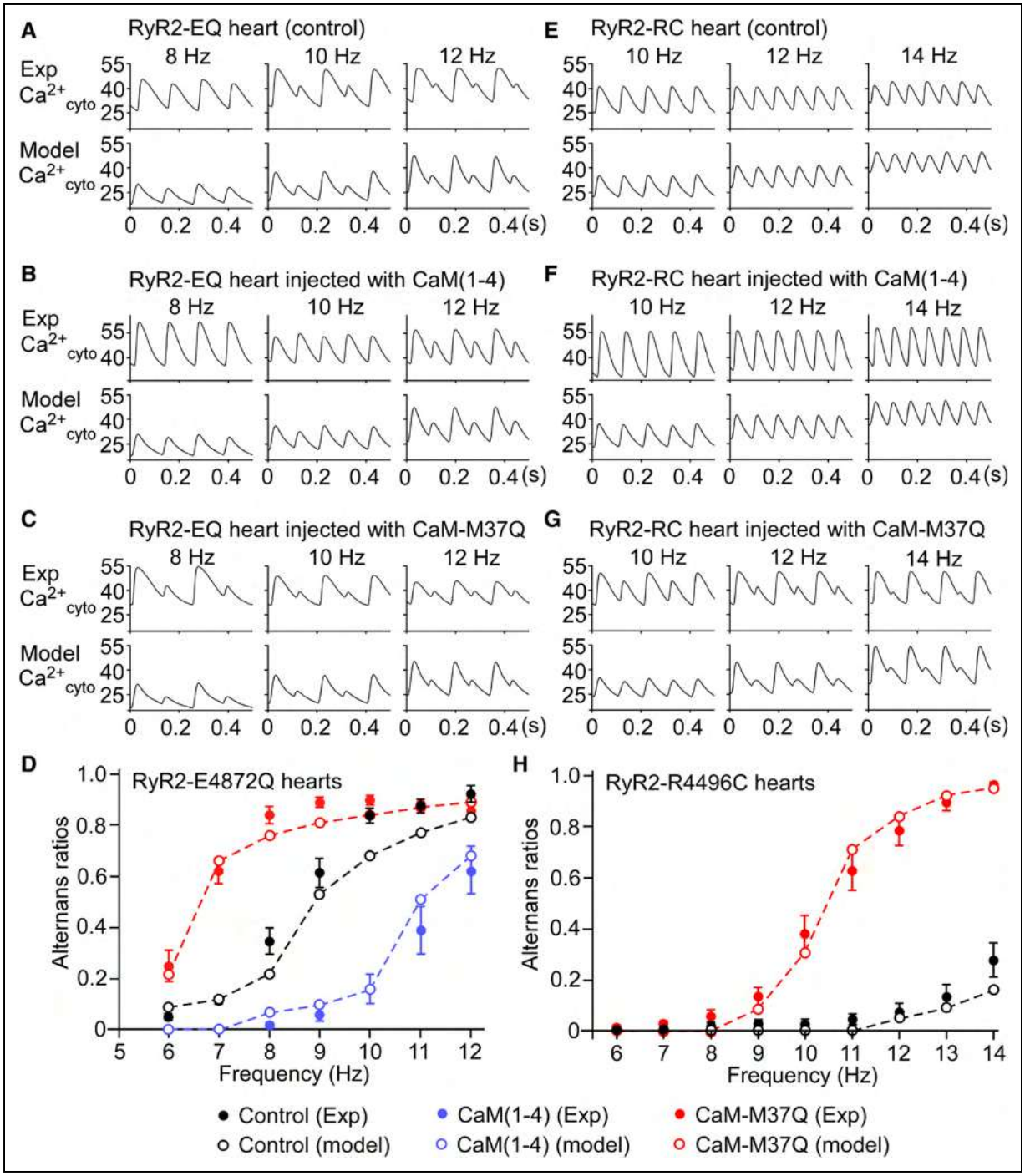

Figure 7. Numerical simulation of altered CaM (calmodulin) function on Ca^{2+} alternans in RyR2 (ryanodine receptor 2)-E4872Q and RyR2-R4496C mutant hearts.

Comparison of numerical and experimental Ca^{2+} traces (concentration of Ca^{2+} bound to Rhod-2) for RyR2-E4872Q (**A**) and RyR2-R4496C (**E**) mutant hearts. The model reproduces very well the dynamics, both in the control case and with injected loss-of-function (LOF) CaM (1–4) (**B** and **F**), and gain-of-function (GOF) CaM-M37Q (**C** and **G**) mutants. The measured amplitudes agree very well in all cases for the RyR2-E4872Q (**D**) and RyR2-R4496C (**H**) mutant hearts.

diastolic fraction of RyR2 available for activation and thus the magnitude of RyR2 mediated Ca^{2+} release and Ca^{2+} transients. As shown in Figure 8C, the diastolic cytosolic Ca^{2+} progressively increased when the S2 stimulation frequency increased from 9 to 10.6 Hz (ie, below the threshold frequency for Ca^{2+} alternans). Given the strict Ca^{2+} dependence of CaM dependent inactivation of RyR2, the diastolic fraction of Ca^{2+}-CaM inactivated RyR2 is expected to increase as a result of increasing diastolic cytosolic Ca^{2+}. That was indeed the case (Figure 8D). Thus, pacing-induced elevation in diastolic cytosolic Ca^{2+} likely triggers Ca^{2+}-CaM dependent inactivation of RyR2.

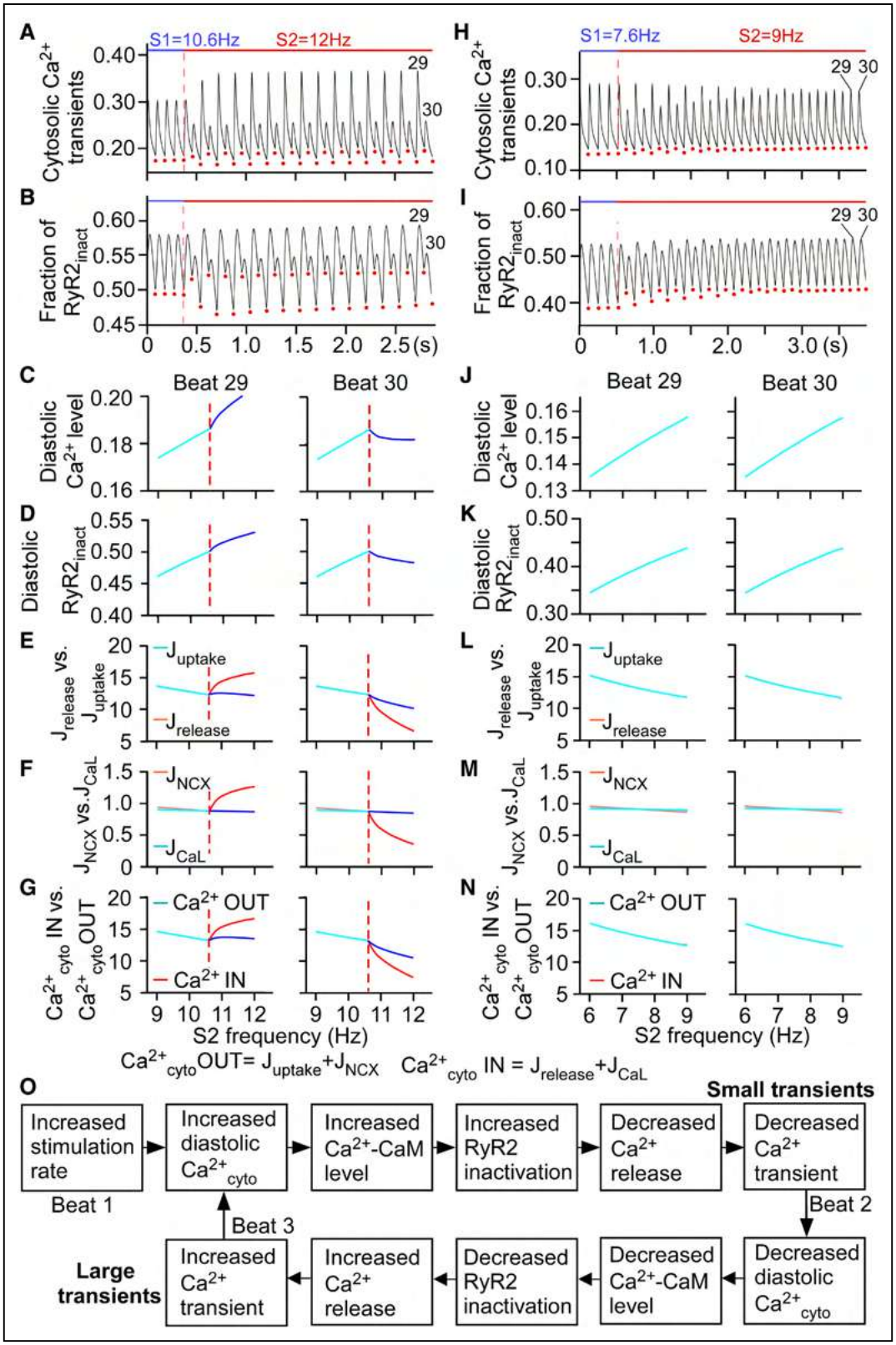

Figure 8. Pacing-induced elevation of diastolic cytosolic Ca^{2+} causes RyR2 (ryanodine receptor 2) inactivation, Ca^{2+} flux imbalance, and Ca^{2+} alternans.

We performed S1-S2 protocols with an S1 frequency at 10.6 Hz, just below the onset of alternans, and with S2 frequencies ranging from 9 to 12 Hz. An example is shown with S2=12 Hz, where alternans develop in both the cytosolic Ca^{2+} transient (**A**) and the fraction of inactivated RyR2 (**B**). We then measured, at each beat after the change in frequency, the diastolic values of cytosolic Ca^{2+} (**C**) and the diastolic fraction of inactivated RyR2 (**D**). For clarity, we indicate with red dots in (**A**) and (**B**) the diastolic points where these values are taken. (*Continued*)

Interestingly, when the S2 stimulation frequency increased to >10.6 Hz (ie, above the alternans threshold frequency), the diastolic cytosolic Ca^{2+} progressively increased at one beat but decreased in the following beat (Figure 8C, beats 29 and 30). Such a beat-to-beat alternation leads to a bifurcation in the diastolic cytosolic Ca^{2+} (increase at odd beats and decrease at even beats; Figure 8A). Similarly, we observed beat-to-beat alternation in the diastolic fraction of inactivated RyR2 (Figure 8D). When the pacing frequency is above the alternans threshold frequency (10.6 Hz), the diastolic fraction of inactivated RyR2 started to bifurcate (Figure 8D, beats 29 and 30), corresponding to the bifurcation in the diastolic cytosolic Ca^{2+}. Thus, these simulations suggest that diastolic cytosolic Ca^{2+} alternations play a key role in diastolic RyR2 inactivation alternations that drive Ca^{2+} alternans.

Diastolic Cytosolic Ca^{2+} Alternation Results From Ca^{2+} Influx-Efflux Imbalance

To further explore why the diastolic cytosolic Ca^{2+} displayed beat-to-beat alternations when the stimulation frequency exceeds the alternans threshold frequency, we analyzed the major Ca^{2+} fluxes that contribute to the homeostasis of cytosolic Ca^{2+} at different pacing frequencies (Figure 8E through 8G). These analyses revealed that the removal of Ca^{2+} out of the cytosol (Ca^{2+}_{cyto}OUT= SR Ca^{2+} uptake [J_{uptake}] + Na^+/Ca^{2+} exchanger mediated Ca^{2+} removal) and the influx of Ca^{2+} into the cytosol (Ca^{2+}_{cyto}IN= RyR2 mediated Ca^{2+} release [$J_{release}$] + L-type Ca^{2+} channel-mediated Ca^{2+} influx) are identical at pacing frequencies below the alternans threshold frequency (<10.6 Hz). However, at the pacing frequencies above the alternans threshold frequency (>10.6 Hz), the removal of Ca^{2+} out of the cytosol (Ca^{2+}_{cyto}OUT) is smaller than the influx of Ca^{2+} into the cytosol (Ca^{2+}_{cyto}IN) at one beat (beat 29, Figure 8E through 8G). This imbalance leads to an elevation in diastolic cytosolic Ca^{2+} and the diastolic fraction of inactivated RyR2 (Figure 8C and 8D, beat 29). In the next beat (beat 30), the situation is reversed; the removal of Ca^{2+} out of the cytosol is greater than the influx of Ca^{2+} into the cytosol at pacing frequencies above the alternans threshold frequency (>10.6 Hz; Figure 8E through 8G, beat 30), leading to a reduction in diastolic cytosolic Ca^{2+} and the diastolic fraction of inactivated RyR2 (Figure 8C and 8D, beat 30). Thus, the imbalance between Ca^{2+} removal from and Ca^{2+} influx into the cytosol causes beat-to-beat alternations in diastolic cytosolic Ca^{2+}, in the diastolic fraction of inactivated RyR2, and thus in RyR2-mediated Ca^{2+} release and in Ca^{2+} transients.

We also analyzed the cytosolic Ca^{2+} transients and the fraction of inactivated RyR2 using stimulation frequencies (S1=7.6 Hz and S2=7.6–9 Hz) below the alternans threshold frequency (<10.6 Hz; Figure 8H through 8N). After the system has stabilized (eg, beats 29 and 30), there are no beat-to-beat alternations in diastolic cytosolic Ca^{2+} or in the diastolic fraction of inactivated RyR2 (Figure 8J and 8K). All Ca^{2+} fluxes are balanced in the steady state (Figure 8L through 8N, beats 29 and 30). Thus, there is no Ca^{2+} alternans when pacing frequency is below the alternans threshold frequency (10.6 Hz), despite the increase in the diastolic cytosolic Ca^{2+} and diastolic fraction of inactivated RyR2 with increasing pacing frequency.

Ca^{2+}-CaM Dependent RyR2 Inactivation Drives Ca^{2+} Flux Imbalance

We next explored what triggers the imbalance of Ca^{2+} fluxes and diastolic cytosolic Ca^{2+} alternation. In cardiomyocytes, the level of diastolic cytosolic Ca^{2+} is largely determined by the L-type Ca^{2+} channel-mediated Ca^{2+} influx, $J_{release}$, J_{uptake}, and Na^+/Ca^{2+} exchanger mediated Ca^{2+} removal. Rapid pacing induces changes in each of these currents (Figure 8E, 8F, 8L, and 8M). Since Ca^{2+} cycling in mouse cardiomyocytes is mainly determined by $J_{release}$ and J_{uptake}, the diastolic cytosolic Ca^{2+} level would be largely determined by $J_{release}$ and J_{uptake}. Moreover, J_{uptake} remains relatively linear in response to increasing pacing frequencies (Figure 8E and 8L). Hence, rapid pacing-induced Ca^{2+} flux imbalance primarily results from the nonlinear changes in $J_{release}$ (Figure 8E and 8G), which is caused by Ca^{2+}-CaM-dependent inactivation of RyR2. Therefore, Ca^{2+}-CaM dependent RyR2 inactivation by affecting $J_{release}$ drives Ca^{2+} flux imbalance, diastolic cytosolic Ca^{2+} alternation, and thus Ca^{2+} alternans.

DISCUSSION

Experimental and mathematical modeling studies have suggested that beat-to-beat alternations in the inactivation/refractoriness of RyR2 play an important role in cardiac Ca^{2+} alternans.[20,33] However, the molecular mechanism underlying RyR2 inactivation/refractoriness remains largely unknown. CaM is known to inhibit RyR2 and promotes termination of RyR2-mediated Ca^{2+}

Figure 8 Continued. We then measured the fluxes corresponding to each beat and integrate the currents over the duration of the beat, corresponding to fluxes across the sarcoplasmic reticulum (SR) by SR Ca^{2+} release ($J_{release}$) or uptake (J_{uptake}; **E**), across the cell membrane by the L-type Ca^{2+} channel (I_{CaL}) and the Na/Ca^{2+} exchanger (I_{NCX}; **F**), and the total Ca^{2+} in or out of the cytosol, as the sum of the previous fluxes (**G**). We also performed S1-S2 protocols with an S1 frequency at 7.6 Hz and S2 frequencies ranging from 6 to 9 Hz (below the alternans threshold frequency). Similarly, we analyzed cytosolic Ca^{2+} transient (**H**), the fraction of inactivated RyR2 (**I**), the diastolic cytosolic Ca^{2+} (**J**), the diastolic fraction of inactivated RyR2 (**K**), the $J_{release}$ and J_{uptake}; **L**), the I_{CaL} and the Na/Ca^{2+} exchanger currents (I_{NCX}; **M**), and the total Ca^{2+} in or out of the cytosol (**N**). **O**, Proposed mechanism for fast pacing-induced Ca^{2+} alternans.

release. CaM also modulates the refractoriness of RyR2-mediated Ca^{2+} release.[34,37,38,44] Therefore, by virtue of its actions on RyR2 inactivation and Ca^{2+} release refractoriness, CaM would play a critical role in Ca^{2+} alternans. To directly test this idea, in the present study, we altered the function of CaM in cardiomyocytes in intact working hearts using adenovirus-mediated gene delivery of CaM mutants in vivo and assessed the impact of CaM mutations on Ca^{2+} transients using in situ intact heart Ca^{2+} imaging. We found that diminishing CaM function (as in CaM [1–4] mutation) shortened the recovery of Ca^{2+} transients and protected against Ca^{2+} alternans. In contrast, enhancing CaM function (as in CaM-M37Q mutation) prolonged the recovery of Ca^{2+} transients and promoted Ca^{2+} alternans. These data demonstrate, for the first time, that CaM is an important determinant of Ca^{2+} alternans in intact hearts.

We have demonstrated previously that activation of RyR2 by SR luminal Ca^{2+} plays an important role in Ca^{2+} alternans.[27,28] Inhibiting RyR2 luminal Ca^{2+} activation promotes Ca^{2+} alternans, whereas enhancing RyR2 luminal Ca^{2+} activation suppresses Ca^{2+} alternans. These effects of altered RyR2 luminal Ca^{2+} regulation on Ca^{2+} alternans are opposite to those of altered CaM function. Hence, Ca^{2+} alternans is likely to be modulated by multiple competing regulators of RyR2, including CaM, luminal Ca^{2+}, and cytosolic Ca^{2+}. To understand this complex interplay, we developed a novel numerical myocyte model that incorporates RyR2 inactivation by Ca^{2+}-CaM as well as RyR2 activation by cytosolic and luminal Ca^{2+} a in a 4-state model of RyR2.[49] Recently, high-resolution 3-dimensional structures of the CaM-RyR2 complexes in the absence and presence of Ca^{2+} have been resolved.[36] These structural analyses indicate that inactivation of RyR2 by CaM requires Ca^{2+} binding to CaM and the binding of the Ca^{2+}-CaM complex to RyR2 and that recovery of RyR2 from Ca^{2+}-CaM-dependent inactivation requires the dissociation of Ca^{2+}-CaM from RyR2. To model this Ca^{2+}-dependent CaM inactivation of RyR2 and its recovery from inactivation, we included an inactivation rate proportional to the concentration of Ca^{2+}-CaM, while the recovery rate is assumed to be constant. For RyR2 activation, we assumed cytosolic Ca^{2+} activation is proportional to the square of the cytosolic Ca^{2+} concentration. Given the steep dependence of RyR2 activation by luminal Ca^{2+}, we modeled luminal Ca^{2+} activation of RyR2 with a large Hill coefficient (n=6). Remarkably, our newly developed model recapitulates not only the impact of altered CaM function but also the impact of altered luminal Ca^{2+} activation of RyR2 on Ca^{2+} alternans under 9 different experimental conditions. This excellent match between experimental and simulation data indicates that Ca^{2+} alternans is largely controlled by the activity of RyR2 and is thus subjected to modulation by RyR2 regulators (cytosolic Ca^{2+}, luminal Ca^{2+}, and CaM).

Although it is well recognized that RyR2 inactivation underlies Ca^{2+} alternans, how RyR2 inactivation induces Ca^{2+} alternans remains largely undefined. Our simulation analyses reveal that the fraction of RyR2 available for stimulated SR Ca^{2+} release is determined by the diastolic fraction of Ca^{2+}-CaM inactivated RyR2, which is in turn determined by the diastolic cytosolic Ca^{2+} level (ie, the level of cytosolic Ca^{2+} just before stimulation). The level of this diastolic cytosolic Ca^{2+} is largely determined by the net balance of $J_{release}$ and J_{uptake}. Increasing the pacing frequency (ie, shortened cycle length) will reduce SR Ca^{2+} uptake, as the SR Ca^{2+} pump has less time to remove cytosolic Ca^{2+}. Reduced SR Ca^{2+} uptake will result in an elevation in diastolic cytosolic Ca^{2+}. However, this pacing-induced elevation in diastolic cytosolic Ca^{2+} will increase the level of the Ca^{2+}-CaM complex and the fraction of Ca^{2+}-CaM inactivated RyR2, which will reduce the fraction of RyR2 available for activation and thus SR Ca^{2+} release. Reduced SR Ca^{2+} release will, in turn, decrease diastolic cytosolic Ca^{2+}. Thus, increasing the pacing frequency has 2 opposing effects on the diastolic cytosolic Ca^{2+} level. It is the net effect of these 2 opposing forces that determine the induction of Ca^{2+} alternans. When the pacing frequency is below the alternans threshold frequency, SR Ca^{2+} uptake equals to SR Ca^{2+} release at the steady state (Figure 8). As such, there are no beat-to-beat alternations in the diastolic cytosolic Ca^{2+}, in RyR2 inactivation, or in RyR2-mediated Ca^{2+} release (ie, no Ca^{2+} alternans). However, when the pacing frequency exceeds the alternans threshold, SR Ca^{2+} uptake is greater than SR Ca^{2+} release at one beat due to strong inactivation of RyR2 by the elevated diastolic cytosolic Ca^{2+}. This will result in a decrease in the diastolic cytosolic Ca^{2+}. The reduction in diastolic cytosolic Ca^{2+} will reduce the Ca^{2+}-CaM complex and thus the Ca^{2+}-CaM-dependent RyR2 inactivation. This reduced RyR2 inactivation will increase SR Ca^{2+} release and diastolic cytosolic Ca^{2+} on the next beat. Thus, increasing pacing frequency above the alternans threshold leads to imbalance of SR Ca^{2+} uptake and Ca^{2+} release, causing beat-to-beat alternations in diastolic cytosolic Ca^{2+}, in RyR2 inactivation, and in RyR2-mediated Ca^{2+} release (ie, Ca^{2+} alternans). Taken together, we propose that rapid pacing-induced Ca^{2+} alternans is caused by a feedback loop in which elevated diastolic cytosolic Ca^{2+} leads to increased Ca^{2+}-CaM-dependent inactivation of RyR2, reduced SR Ca^{2+} release, SR Ca^{2+} release-uptake imbalance, and decreased diastolic cytosolic Ca^{2+} (Figure 8). This diastolic cytosolic Ca^{2+} alternation then drives diastolic RyR2 inactivation alternation and Ca^{2+} alternans.

Although cytosolic Ca^{2+} has been suggested in the induction of Ca^{2+} alternans, the role of cytosolic Ca^{2+} in Ca^{2+} alternans and its underlying mechanism is unclear and controversial. Early modeling studies assumed the presence of cytosolic Ca^{2+} dependent-inactivation of RyR2 in simulating Ca^{2+} alternans.[49] However, this is not

universally accepted because in vitro experiments, cytosolic Ca^{2+} in the physiological range does not provide sufficient inactivation of RyR2. Rather, other mechanisms of RyR2 termination have been proposed, such as SR Ca^{2+} depletion or stochastic attrition.[50,51] Nevertheless, in vivo experiments[52] seem to support the idea of a strong inactivation of RyR2 by cytosolic Ca^{2+}. Following these ideas, RyR2 inactivation has been proposed as a possible mechanism for alternans both in modeling[20,32,33] and in experimental studies.[16,23,27,29,30] These studies shed light on how an incomplete recovery of RyR2 from inactivation (or refractoriness) can lead to alternans at fast pacing rates. However, the mechanism of RyR2 inactivation and its relation to the pacing rate are completely undefined. It is this crucial point that the present study has addressed. We demonstrate that pacing-induced cytosolic Ca^{2+} elevation increases the Ca^{2+}-CaM complex that induces RyR2 inactivation that drives Ca^{2+} alternans.

Given its significant role in modulating SR Ca^{2+} release, impaired CaM function is expected to be pathological. Indeed, naturally occurring mutations in CaM cause cardiac arrhythmias and sudden death.[53] Impairing CaM inhibition of RyR2 in mice by mutating the CaM binding site in RyR2 also causes cardiac hypertrophy and early death.[54] Reduced CaM binding to RyR2 has also been implicated in heart failure.[35,55] Thus, these observations suggest that enhancing CaM-RyR2 interaction may represent an effective therapeutic strategy for treating cardiac arrhythmias and heart failure. In support of this idea, it has recently been shown that the GOF CaM-M37Q mutation and enhancing CaM-RyR2 interaction are able to suppress spontaneous SR Ca^{2+} release and catecholaminergic polymorphic ventricular tachycardia.[44] However, as shown in the present study, enhancing CaM function (as in CaM-M37Q mutation) markedly promotes Ca^{2+} alternans that can lead to ventricular fibrillation and sudden death. Given that both enhancing and suppressing CaM function could lead to cardiac arrhythmias, normalizing the activity of CaM would be the key in protecting against CaM-mediated cardiac arrhythmias.

The impact of CaM and CaM mutations on Ca^{2+} dynamics/fluxes in isolated cardiomyocytes has been extensively investigated.[38,44,56–60] Surprisingly, little is known about the impact of CaM and CaM mutations on Ca^{2+} alternans. This is due, in part, to the technical difficulties of studying the effects of altered CaM function on Ca^{2+} alternans in isolated cardiomyocytes or in intact hearts. It is generally difficult to induce stable Ca^{2+} alternans in isolated cultured cardiomyocytes overexpressing CaM or CaM mutants at physiologically relevant pacing frequencies. It is also difficult to study the impact of altered CaM function globally in the intact heart without detrimental effects, given its critical roles in many cellular processes. To circumvent the problems associated with isolated cultured cardiomyocytes and global adverse effects on the heart, we used a local in vivo gene delivery approach by directly injecting adenoviruses expressing CaM or CaM mutants into the anterior wall of the left ventricle. This local expression allows us to assess, for the first time, the impact of altered CaM function on Ca^{2+} alternans and Ca^{2+} transient recovery in cardiomyocytes in the setting of intact hearts. Furthermore, there is evidence suggesting that the induction and mechanism of fast-pacing induced Ca^{2+} alternans in single isolated cardiomyocytes may be different from those in intact hearts. For instance, enhanced RyR2 function has been shown to promote Ca^{2+} alternans in isolated cardiomyocytes where spontaneous Ca^{2+} release events are present.[61–63] In contrast, we showed that enhanced RyR2 function suppresses Ca^{2+} alternans in intact working hearts.[28] Although the exact reason for this difference has yet to be determined, one clear difference between isolated cardiomyocytes and intact hearts is the lack of spontaneous Ca^{2+} release events in intact hearts during fast-pacing that induces Ca^{2+} alternans.[28] Moreover, the stimulation frequency required to trigger Ca^{2+} alternans in intact hearts is much higher than that in isolated cardiomyocytes. These observations suggest that the mechanism that contributes to fast-pacing induced Ca^{2+} alternans in intact hearts may be different from that in isolated cardiomyocytes. Thus, our local in vivo gene delivery technique combined with in situ intact heart Ca^{2+} imaging represents a more physiologically relevant approach to investigating the role of CaM in Ca^{2+} alternans as compared with the single-cell approach.

In summary, the present study demonstrates that Ca^{2+}-CaM-dependent inactivation of RyR2 plays an important role in pacing-induced Ca^{2+} alternans in intact hearts. Based on our new findings, we developed a novel numerical myocyte model of Ca^{2+} alternans. The new model recapitulates the impact of altered RyR2 and CaM function on Ca^{2+} alternans under 9 different experimental conditions. Our simulation analyses reveal that pacing-induced diastolic cytosolic Ca^{2+} elevation drives Ca^{2+}-CaM-dependent RyR2 inactivation and that RyR2 inactivation, when sufficiently high, leads to SR Ca^{2+} release-uptake imbalance. This imbalanced Ca^{2+} uptake and release results in alternations in diastolic cytosolic Ca^{2+}, in RyR2 inactivation, and in SR Ca^{2+} release, and thus perpetuation of Ca^{2+} alternans.

STUDY LIMITATIONS

Despite the physiological advantages of in vivo CaM manipulation and in situ intact heart imaging, our intact heart imaging approach does not isolate the effects of altered CaM function on specific CaM targets. Therefore, although RyR2 is a major target of CaM regulation of Ca^{2+} alternans, it is likely that other CaM targets are importantly involved as well. Further studies will be needed to fully understand the roles of different CaM targets in Ca^{2+} alternans in the setting of intact hearts. Given the close coupling between Ca^{2+} alternans and APD alternans, the

role of CaM in APD alternans has yet to be determined. Furthermore, since a mathematical model cannot be used as a definitive proof of a biological function, the fact that our mathematical model reproduces very well the experimental data and supports the notion that CaM-dependent inactivation of RyR2 is a key determinant of Ca^{2+} alternans does not entirely rule out that a variation of the model might also agree with the experiments and explain Ca^{2+} alternans by a different mechanism. An interesting observation in our simulations is that pacing at 9 Hz led to transient alternans while pacing at 12 Hz resulted in stable alternans. However, more studies will be required to fully understand the mechanism underlying transient and stable Ca^{2+} alternans at different stimulation frequencies.

ARTICLE INFORMATION

Received October 21, 2020; revision received December 22, 2020; accepted December 29, 2020.

Affiliations

Department of Physiology and Pharmacology, Libin Cardiovascular Institute, University of Calgary, Alberta, Canada (J.W., J.Y., D.B., W.G., X.Z., B.S., R.W., J.P.E., S.R.W.C.). Department of Automatic Control, Universitat Politècnica de Catalunya, Barcelona, Spain (A.V., R.B.). Institut de Recerca Sant Joan de Déu (IRSJD), Barcelona, Spain (R.B.). Biomedical Research Institute Barcelona IIBB-CSIC, CIBERCV and IIB Sant Pau, Hospital de Sant Pau, Barcelona, Spain (L.H.-M.). Department of Physics, Universitat Politècnica de Catalunya, Barcelona, Spain (E.A.-L., B.E.).

Acknowledgments

This work was supported by research grants from the Heart and Stroke Foundation of Canada (G-19-0026444), the Heart and Stroke Foundation Chair in Cardiovascular Research (END611955), the Canadian Institutes of Health Research to S.R.W. Chen (PJT-155940), the Spanish Ministry of Science Innovation and Universities SAF2017-88019-C3-1R, 2R, and 3R (to L. Hove-Madsen, R. Benitez, and B. Echebarria), Marato-TV3 20152030 (to L. Hove-Madsen) and 20151110 (to B. Echebarria), and Generalitat de Catalunya SGR2017-1769 (to L. Hove-Madsen). J. Wei, J. Yao, D. Belke, W. Guo, X. Zhong, B. Sun, R. Benitez, L. Hove-Madsen, E. Alvarez-Lacalle, B. Echebarria, and S.R.W. Chen designed the research. J. Wei, J. Yao, D. Belke, W. Guo, X. Zhong, B. Sun, R. Wang, J. Paul Estillore, A. Vallmitjana, E. Alvarez-Lacalle, and B. Echebarria performed the research. J. Wei, J. Yao, D. Belke, W. Guo, X. Zhong, B. Sun, A. Vallmitjana, R. Benitez, L. Hove-Madsen, E. Alvarez-Lacalle, B. Echebarria, and S.R.W. Chen analyzed data. J. Wei, J. Yao, D. Belke, L. Hove-Madsen, E. Alvarez-Lacalle, B. Echebarria, and S.R.W. Chen wrote the article.

Sources of Funding

None.

Disclosures

J. Wei, recipient of the Libin Cardiovascular Institute and Cumming School of Medicine Postdoctoral Fellowship Award. J. Yao and B. Sun, recipients of the Alberta Innovates-Health Solutions (AIHS) Fellowship Award. X. Zhong and W. Guo, recipients of the Alberta Innovates-Health Solutions (AIHS) Studentship Award. S.R.W. Chen, AIHS Scientist. The other authors report no conflicts.

Supplemental Materials

Expanded Materials and Methods
Online Tables I–IV
Online Figures I–VII
References 64–71

REFERENCES

1. Kapur S, Wasserstrom JA, Kelly JE, Kadish AH, Aistrup GL. Acidosis and ischemia increase cellular Ca2+ transient alternans and repolarization alternans susceptibility in the intact rat heart. *Am J Physiol Heart Circ Physiol.* 2009;296:H1491–H1512. doi: 10.1152/ajpheart.00539.2008
2. Wilson LD, Jeyaraj D, Wan X, Hoeker GS, Said TH, Gittinger M, Laurita KR, Rosenbaum DS. Heart failure enhances susceptibility to arrhythmogenic cardiac alternans. *Heart Rhythm.* 2009;6:251–259. doi: 10.1016/j.hrthm.2008.11.008
3. Giudici MC, Savage MP. Transient pulsus alternans during acute myocardial ischemia and its resolution following beta-adrenergic blockade. *Am Heart J.* 1990;119:960–962. doi: 10.1016/s0002-8703(05)80340-0
4. Verrier RL, Nearing BD. Electrophysiologic basis for T wave alternans as an index of vulnerability to ventricular fibrillation. *J Cardiovasc Electrophysiol.* 1994;5:445–461. doi: 10.1111/j.1540-8167.1994.tb01184.x
5. Rosenbaum DS, Jackson LE, Smith JM, Garan H, Ruskin JN, Cohen RJ. Electrical alternans and vulnerability to ventricular arrhythmias. *N Engl J Med.* 1994;330:235–241. doi: 10.1056/NEJM199401273300402
6. Escobar AL, Valdivia HH. Cardiac alternans and ventricular fibrillation: a bad case of ryanodine receptors reneging on their duty. *Circ Res.* 2014;114:1369–1371. doi: 10.1161/CIRCRESAHA.114.303823
7. Kihara Y, Morgan JP. Abnormal Cai2+ handling is the primary cause of mechanical alternans: study in ferret ventricular muscles. *Am J Physiol.* 1991;261:H1746–H1755. doi: 10.1152/ajpheart.1991.261.6.H1746
8. Chudin E, Goldhaber J, Garfinkel A, Weiss J, Kogan B. Intracellular Ca(2+) dynamics and the stability of ventricular tachycardia. *Biophys J.* 1999;77:2930–2941. doi: 10.1016/S0006-3495(99)77126-2
9. Díaz ME, O'Neill SC, Eisner DA. Sarcoplasmic reticulum calcium content fluctuation is the key to cardiac alternans. *Circ Res.* 2004;94:650–656. doi: 10.1161/01.RES.0000119923.64774.72
10. Laurita KR, Rosenbaum DS. Cellular mechanisms of arrhythmogenic cardiac alternans. *Prog Biophys Mol Biol.* 2008;97:332–347. doi: 10.1016/j.pbiomolbio.2008.02.014
11. Xie LH, Sato D, Garfinkel A, Qu Z, Weiss JN. Intracellular Ca alternans: coordinated regulation by sarcoplasmic reticulum release, uptake, and leak. *Biophys J.* 2008;95:3100–3110. doi: 10.1529/biophysj.108.130955
12. Aistrup GL, Shiferaw Y, Kapur S, Kadish AH, Wasserstrom JA. Mechanisms underlying the formation and dynamics of subcellular calcium alternans in the intact rat heart. *Circ Res.* 2009;104:639–649. doi: 10.1161/CIRCRESAHA.108.181909
13. Wan X, Laurita KR, Pruvot EJ, Rosenbaum DS. Molecular correlates of repolarization alternans in cardiac myocytes. *J Mol Cell Cardiol.* 2005;39:419–428. doi: 10.1016/j.yjmcc.2005.06.004
14. Eisner DA, Li Y, O'Neill SC. Alternans of intracellular calcium: mechanism and significance. *Heart Rhythm.* 2006;3:743–745. doi: 10.1016/j.hrthm.2005.12.020
15. Laurita KR, Rosenbaum DS. Mechanisms and potential therapeutic targets for ventricular arrhythmias associated with impaired cardiac calcium cycling. *J Mol Cell Cardiol.* 2008;44:31–43. doi: 10.1016/j.yjmcc.2007.10.012
16. Wang L, Myles RC, De Jesus NM, Ohlendorf AK, Bers DM, Ripplinger CM. Optical mapping of sarcoplasmic reticulum Ca2+ in the intact heart: ryanodine receptor refractoriness during alternans and fibrillation. *Circ Res.* 2014;114:1410–1421. doi: 10.1161/CIRCRESAHA.114.302505
17. Kanaporis G, Blatter LA. The mechanisms of calcium cycling and action potential dynamics in cardiac alternans. *Circ Res.* 2015;116:846–856. doi: 10.1161/CIRCRESAHA.116.305404
18. Bers DM. Cardiac excitation-contraction coupling. *Nature.* 2002;415:198–205. doi: 10.1038/415198a
19. Cordeiro JM, Malone JE, Di Diego JM, Scornik FS, Aistrup GL, Antzelevitch C, Wasserstrom JA. Cellular and subcellular alternans in the canine left ventricle. *Am J Physiol Heart Circ Physiol.* 2007;293:H3506–H3516. doi: 10.1152/ajpheart.00757.2007
20. Alvarez-Lacalle E, Cantalapiedra IR, Peñaranda A, Cinca J, Hove-Madsen L, Echebarria B. Dependency of calcium alternans on ryanodine receptor refractoriness. *PLoS One.* 2013;8:e55042. doi: 10.1371/journal.pone.0055042
21. Qu Z, Liu MB, Nivala M. A unified theory of calcium alternans in ventricular myocytes. *Sci Rep.* 2016;6:35625. doi: 10.1038/srep35625
22. Hüser J, Wang YG, Sheehan KA, Cifuentes F, Lipsius SL, Blatter LA. Functional coupling between glycolysis and excitation-contraction coupling underlies alternans in cat heart cells. *J Physiol.* 2000;524 Pt 3:795–806. doi: 10.1111/j.1469-7793.2000.00795.x
23. Picht E, DeSantiago J, Blatter LA, Bers DM. Cardiac alternans do not rely on diastolic sarcoplasmic reticulum calcium content fluctuations. *Circ Res.* 2006;99:740–748. doi: 10.1161/01.RES.0000244002.88813.91
24. Llach A, Molina CE, Fernandes J, Padró J, Cinca J, Hove-Madsen L. Sarcoplasmic reticulum and L-type Ca^{2+} channel activity regulate the beat-to-beat stability of calcium handling in human atrial myocytes. *J Physiol.* 2011;589:3247–3262. doi: 10.1113/jphysiol.2010.197715
25. Molina CE, Llach A, Herraiz-Martínez A, Tarifa C, Barriga M, Wiegerinck RF, Fernandes J, Cabello N, Vallmitjana A, Benitéz R, et al. Prevention

of adenosine A2A receptor activation diminishes beat-to-beat alternation in human atrial myocytes. *Basic Res Cardiol.* 2016;111:5. doi: 10.1007/s00395-015-0525-2
26. Díaz ME, Eisner DA, O'Neill SC. Depressed ryanodine receptor activity increases variability and duration of the systolic Ca2+ transient in rat ventricular myocytes. *Circ Res.* 2002;91:585–593. doi: 10.1161/01.res.0000035527.53514.c2
27. Zhong X, Sun B, Vallmitjana A, Mi T, Guo W, Ni M, Wang R, Guo A, Duff HJ, Gillis AM, et al. Suppression of ryanodine receptor function prolongs Ca2+ release refractoriness and promotes cardiac alternans in intact hearts. *Biochem J.* 2016;473:3951–3964. doi: 10.1042/BCJ20160606
28. Sun B, Wei J, Zhong X, Guo W, Yao J, Wang R, Vallmitjana A, Benitez R, Hove-Madsen L, Chen SRW. The cardiac ryanodine receptor, but not sarcoplasmic reticulum Ca2+-ATPase, is a major determinant of Ca2+ alternans in intact mouse hearts. *J Biol Chem.* 2018;293:13650–13661.
29. Shkryl VM, Maxwell JT, Domeier TL, Blatter LA. Refractoriness of sarcoplasmic reticulum Ca2+ release determines Ca2+ alternans in atrial myocytes. *Am J Physiol Heart Circ Physiol.* 2012;302:H2310–H2320. doi: 10.1152/ajpheart.00079.2012
30. Lugo CA, Cantalapiedra IR, Peñaranda A, Hove-Madsen L, Echebarria B. Are SR Ca content fluctuations or SR refractoriness the key to atrial cardiac alternans?: insights from a human atrial model. *Am J Physiol Heart Circ Physiol.* 2014;306:H1540–H1552. doi: 10.1152/ajpheart.00515.2013
31. Restrepo JG, Weiss JN, Karma A. Calsequestrin-mediated mechanism for cellular calcium transient alternans. *Biophys J.* 2008;95:3767–3789. doi: 10.1529/biophysj.108.130419
32. Rovetti R, Cui X, Garfinkel A, Weiss JN, Qu Z. Spark-induced sparks as a mechanism of intracellular calcium alternans in cardiac myocytes. *Circ Res.* 2010;106:1582–1591. doi: 10.1161/CIRCRESAHA.109.213975
33. Cantalapiedra IR, Alvarez-Lacalle E, Peñaranda A, Echebarria B. Minimal model for calcium alternans due to SR release refractoriness. *Chaos.* 2017;27:093928. doi: 10.1063/1.5000709
34. Yamaguchi N, Xu L, Pasek DA, Evans KE, Meissner G. Molecular basis of calmodulin binding to cardiac muscle Ca(2+) release channel (ryanodine receptor). *J Biol Chem.* 2003;278:23480–23486. doi: 10.1074/jbc.M301125200
35. Yang Y, Guo T, Oda T, Chakraborty A, Chen L, Uchinoumi H, Knowlton AA, Fruen BR, Cornea RL, Meissner G, et al. Cardiac myocyte Z-line calmodulin is mainly RyR2-bound, and reduction is arrhythmogenic and occurs in heart failure. *Circ Res.* 2014;114:295–306. doi: 10.1161/CIRCRESAHA.114.302857
36. Gong D, Chi X, Wei J, Zhou G, Huang G, Zhang L, Wang R, Lei J, Chen SRW, Yan N. Modulation of cardiac ryanodine receptor 2 by calmodulin. *Nature.* 2019;572:347–351. doi: 10.1038/s41586-019-1377-y
37. Tian X, Tang Y, Liu Y, Wang R, Chen SR. Calmodulin modulates the termination threshold for cardiac ryanodine receptor-mediated Ca2+ release. *Biochem J.* 2013;455:367–375. doi: 10.1042/BJ20130805
38. Kryshtal DO, Gryshchenko O, Gomez-Hurtado N, Knollmann BC. Impaired calcium-calmodulin-dependent inactivation of Cav1.2 contributes to loss of sarcoplasmic reticulum calcium release refractoriness in mice lacking calsequestrin 2. *J Mol Cell Cardiol.* 2015;82:75–83. doi: 10.1016/j.yjmcc.2015.02.027
39. Belke DD, Gloss B, Hollander JM, Swanson EA, Duplain H, Dillmann WH. In vivo gene delivery of HSP70i by adenovirus and adeno-associated virus preserves contractile function in mouse heart following ischemia-reperfusion. *Am J Physiol Heart Circ Physiol.* 2006;291:H2905–H2910. doi: 10.1152/ajpheart.00323.2006
40. Chen B, Guo A, Gao Z, Wei S, Xie YP, Chen SR, Anderson ME, Song LS. In situ confocal imaging in intact heart reveals stress-induced Ca2+ release variability in a murine catecholaminergic polymorphic ventricular tachycardia model of type 2 ryanodine receptor(R4496C+/-) mutation. *Circ Arrhythm Electrophysiol.* 2012;5:841–849.
41. Bai Y, Jones PP, Guo J, Zhong X, Clark RB, Zhou Q, Wang R, Vallmitjana A, Benitez R, Hove-Madsen L, et al. Phospholamban knockout breaks arrhythmogenic Ca^{2+} waves and suppresses catecholaminergic polymorphic ventricular tachycardia in mice. *Circ Res.* 2013;113:517–526. doi: 10.1161/CIRCRESAHA.113.301678
42. Zhang PC, Llach A, Sheng XY, Hove-Madsen L, Tibbits GF. Calcium handling in zebrafish ventricular myocytes. *Am J Physiol Regul Integr Comp Physiol.* 2011;300:R56–R66. doi: 10.1152/ajpregu.00377.2010
43. Bondarenko VE, Szigeti GP, Bett GC, Kim SJ, Rasmusson RL. Computer model of action potential of mouse ventricular myocytes. *Am J Physiol Heart Circ Physiol.* 2004;287:H1378–H1403. doi: 10.1152/ajpheart.00185.2003
44. Liu B, Walton SD, Ho HT, Belevych AE, Tikunova SB, Bonilla I, Shettigar V, Knollmann BC, Priori SG, Volpe P, et al. Gene transfer of engineered calmodulin alleviates ventricular arrhythmias in a calsequestrin-associated mouse model of catecholaminergic polymorphic ventricular tachycardia. *J Am Heart Assoc.* 2018;7:e008155.
45. Gomez-Hurtado N, Boczek NJ, Kryshtal DO, Johnson CN, Sun J, Nitu FR, Cornea RL, Chazin WJ, Calvert ML, Tester DJ, et al. Novel CPVT-associated calmodulin mutation in CALM3 (CALM3-A103V) activates arrhythmogenic Ca waves and sparks. *Circ Arrhythm Electrophysiol.* 2016;9:10.1161/CIRCEP.116.004161 e004161.
46. Peterson BZ, DeMaria CD, Adelman JP, Yue DT. Calmodulin is the Ca2+ sensor for Ca2+ -dependent inactivation of L-type calcium channels. *Neuron.* 1999;22:549–558. doi: 10.1016/s0896-6273(00)80709-6
47. Chen W, Wang R, Chen B, Zhong X, Kong H, Bai Y, Zhou Q, Xie C, Zhang J, Guo A, et al. The ryanodine receptor store-sensing gate controls Ca2+ waves and Ca2+-triggered arrhythmias. *Nat Med.* 2014;20:184–192. doi: 10.1038/nm.3440
48. Jiang D, Xiao B, Yang D, Wang R, Choi P, Zhang L, Cheng H, Chen SR. RyR2 mutations linked to ventricular tachycardia and sudden death reduce the threshold for store-overload-induced Ca2+ release (SOICR). *Proc Natl Acad Sci U S A.* 2004;101:13062–13067. doi: 10.1073/pnas.0402388101
49. Stern MD, Song LS, Cheng H, Sham JS, Yang HT, Boheler KR, Ríos E. Local control models of cardiac excitation-contraction coupling. A possible role for allosteric interactions between ryanodine receptors. *J Gen Physiol.* 1999;113:469–489. doi: 10.1085/jgp.113.3.469
50. Lukyanenko V, Wiesner TF, Gyorke S. Termination of Ca2+ release during Ca2+ sparks in rat ventricular myocytes. *J Physiol.* 1998;507 (pt 3):667–677. doi: 10.1111/j.1469-7793.1998.667bs.x
51. Stern MD, Cheng H. Putting out the fire: what terminates calcium-induced calcium release in cardiac muscle? *Cell Calcium.* 2004;35:591–601. doi: 10.1016/j.ceca.2004.01.013
52. Sham JS, Song LS, Chen Y, Deng LH, Stern MD, Lakatta EG, Cheng H. Termination of Ca2+ release by a local inactivation of ryanodine receptors in cardiac myocytes. *Proc Natl Acad Sci U S A.* 1998;95:15096–15101. doi: 10.1073/pnas.95.25.15096
53. Nyegaard M, Overgaard MT, Søndergaard MT, Vranas M, Behr ER, Hildebrandt LL, Lund J, Hedley PL, Camm AJ, Wettrell G, et al. Mutations in calmodulin cause ventricular tachycardia and sudden cardiac death. *Am J Hum Genet.* 2012;91:703–712. doi: 10.1016/j.ajhg.2012.08.015
54. Yamaguchi N, Takahashi N, Xu L, Smithies O, Meissner G. Early cardiac hypertrophy in mice with impaired calmodulin regulation of cardiac muscle Ca release channel. *J Clin Invest.* 2007;117:1344–1353. doi: 10.1172/JCI29515
55. Ono M, Yano M, Hino A, Suetomi T, Xu X, Susa T, Uchinoumi H, Tateishi H, Oda T, Okuda S, et al. Dissociation of calmodulin from cardiac ryanodine receptor causes aberrant Ca(2+) release in heart failure. *Cardiovasc Res.* 2010;87:609–617. doi: 10.1093/cvr/cvq108
56. Zühlke RD, Pitt GS, Deisseroth K, Tsien RW, Reuter H. Calmodulin supports both inactivation and facilitation of L-type calcium channels. *Nature.* 1999;399:159–162. doi: 10.1038/20200
57. Alseikhan BA, DeMaria CD, Colecraft HM, Yue DT. Engineered calmodulins reveal the unexpected eminence of Ca2+ channel inactivation in controlling heart excitation. *Proc Natl Acad Sci U S A.* 2002;99:17185–17190. doi: 10.1073/pnas.262372999
58. Yang D, Song LS, Zhu WZ, Chakir K, Wang W, Wu C, Wang Y, Xiao RP, Chen SR, Cheng H. Calmodulin regulation of excitation-contraction coupling in cardiac myocytes. *Circ Res.* 2003;92:659–667. doi: 10.1161/01.RES.0000064566.91495.0C
59. Boczek NJ, Gomez-Hurtado N, Ye D, Calvert ML, Tester DJ, Kryshtal D, Hwang HS, Johnson CN, Chazin WJ, Loporcaro CG, et al. Spectrum and prevalence of CALM1-, CALM2-, and CALM3-encoded calmodulin variants in long QT syndrome and functional characterization of a novel long QT syndrome-associated calmodulin missense variant, E141G. *Circ Cardiovasc Genet.* 2016;9:136–146. doi: 10.1161/CIRCGENETICS.115.001323
60. Limpitikul WB, Dick IE, Tester DJ, Boczek NJ, Limphong P, Yang W, Choi MH, Babich J, DiSilvestre D, Kanter RJ, et al. A precision medicine approach to the rescue of function on malignant calmodulinopathic long-QT syndrome. *Circ Res.* 2017;120:39–48. doi: 10.1161/CIRCRESAHA.116.309283
61. Belevych AE, Terentyev D, Viatchenko-Karpinski S, Terentyeva R, Sridhar A, Nishijima Y, Wilson LD, Cardounel AJ, Laurita KR, Carnes CA, et al. Redox modification of ryanodine receptors underlies calcium alternans in a canine

model of sudden cardiac death. *Cardiovasc Res.* 2009;84:387–395. doi: 10.1093/cvr/cvp246
62. Xie W, Santulli G, Guo X, Gao M, Chen BX, Marks AR. Imaging atrial arrhythmic intracellular calcium in intact heart. *J Mol Cell Cardiol.* 2013;64:120–123. doi: 10.1016/j.yjmcc.2013.09.003
63. Kang G, Giovannone SF, Liu N, Liu FY, Zhang J, Priori SG, Fishman GI. Purkinje cells from RyR2 mutant mice are highly arrhythmogenic but responsive to targeted therapy. *Circ Res.* 2010;107:512–519. doi: 10.1161/CIRCRESAHA.110.221481
64. Sikkel MB, Francis DP, Howard J, Gordon F, Rowlands C, Peters NS, Lyon AR, Harding SE, MacLeod KT. Hierarchical statistical techniques are necessary to draw reliable conclusions from analysis of isolated cardiomyocyte studies. *Cardiovasc Res.* 2017;113:1743–1752. doi: 10.1093/cvr/cvx151
65. Zhou Q, Xiao J, Jiang D, Wang R, Vembaiyan K, Wang A, Smith CD, Xie C, Chen W, Zhang J, et al. Carvedilol and its new analogs suppress arrhythmogenic store overload-induced Ca2+ release. *Nat Med.* 2011;17:1003–1009. doi: 10.1038/nm.2406
66. Jiang D, Xiao B, Zhang L, Chen SR. Enhanced basal activity of a cardiac Ca2+ release channel (ryanodine receptor) mutant associated with ventricular tachycardia and sudden death. *Circ Res.* 2002;91:218–225. doi: 10.1161/01.res.0000028455.36940.5e
67. Keizer J, Levine L. Ryanodine receptor adaptation and Ca2+(-)induced Ca2+ release-dependent Ca2+ oscillations. *Biophys J.* 1996;71:3477–3487. doi: 10.1016/S0006-3495(96)79543-7
68. Jafri MS, Rice JJ, Winslow RL. Cardiac Ca2+ dynamics: the roles of ryanodine receptor adaptation and sarcoplasmic reticulum load. *Biophys J.* 1998;74:1149–1168. doi: 10.1016/S0006-3495(98)77832-4
69. Jones PP, Guo W, Chen SRW. Control of cardiac ryanodine receptor by sarcoplasmic reticulum luminal Ca2. *J Gen Physiol.* 2017;149:867–875. doi: 10.1085/jgp.201711805
70. Shannon TR, Ginsburg KS, Bers DM. Potentiation of fractional sarcoplasmic reticulum calcium release by total and free intra-sarcoplasmic reticulum calcium concentration. *Biophys J.* 2000;78:334–343. doi: 10.1016/S0006-3495(00)76596-9
71. Cortassa S, Aon MA, O'Rourke B, Jacques R, Tseng HJ, Marbán E, Winslow RL. A computational model integrating electrophysiology, contraction, and mitochondrial bioenergetics in the ventricular myocyte. *Biophys J.* 2006;91:1564–1589. doi: 10.1529/biophysj.105.076174